SMS

Improving Management Effectiveness Through Computer Technology

DESIGN STUDY OF A LOW BIT RATE TRANSMITTER AND SIMULATOR

January 13, 1972

By F. S. Zusman and P. J. Steen

SCIENTIFIC MANAGEMENT SYSTEMS, INC.

an affiliate of **Resource Management Corporation**

7910 Woodmont Avenue Bethesda, Maryland 20014

DESIGN STUDY OF A LOW BIT RATE TRANSMITTER AND SIMULATOR

January 13, 1972

By F. S. Zusman & P. J. Steen

Prepared by Scientific Management Systems, Inc. (SMS)
Under Contract NAS5-11480 For The National Aeronautics and Space Administration
Goddard Space Flight Center, Greenbelt, Maryland 20771

SCIENTIFIC MANAGEMENT SYSTEMS, INC. 7910 Woodmont Avenue, Bethesda, Maryland 20014

PREFACE

This report was prepared under study Contract NAS5-11480, "Design Study of a Low Bit Rate Transmitter and Simulator," by Scientific Management Systems, Inc. The study was sponsored by the National Aeronautics and Space Administration under the direction of Richard L. Kutz.

The purpose of this study was to establish a baseline communications channel model to study low bit rate telemetry transmissions from a Venus Planetary Explorer Spacecraft. The approach taken was to implement existing models drawn from studies conducted by the Jet Propulsion Laboratories (JPL) and once these existing baseline simulation models were implemented and running on NASA/GSFC computers new and original concepts were to be added onto the baseline model as the Planetary Explorer Program requirements dictated. Subsequent to the completion of this study the Planetary Explorer Program was transferred to Ames Research Center and the urgent requirements of this study have diminished. Consequently this report presents the results achieved prior to the termination of the Planetary Explorer Project at NASA/GSFC.

TABLE OF CONTENTS

LIST OF FIGURES

LIST OF FIGURES (Continued)

LIST OF TABLES

INTRODUCTION

1.1 GENERAL

This report describes the results achieved to date in developing a simulation model of the Planetary Explorer Small Probe Communications Links. The results described are the first step in developing an overall model to be used as a test for evaluation of design alternatives for the PE communications subsystems.

1.2 SIMULATION MODEL

1.2.1 General

The construction of appropriate mathematical models for physical sources and channels must be guided by the intended use of the finished product. It was decided to initially develop a model based upon low data rate signals which are recovered by spectral analysis using FFT techniques with signal acquisition and tracking being accomplished using a method implemented by JPL. Subsequent modifications and additions to the baseline simulation will be accomplished on an as required basis as dictated by required design tradeoffs.

Figure 1.1 presents a block diagram of a communications system slanted toward information theoretic considerations.[1/] These considerations when correlated with hardware considerations will provide a basis for detailed hardware design. The scope of this initial effort is limited to those blocks included in the dashed lines. Subsequent paragraphs describe the overall simulation concept with details for the discrete channel presented in section 2.

1/ Information Theory & Reliable Communication, by R. G. Gallager, 1968, John Wiley & Sons.

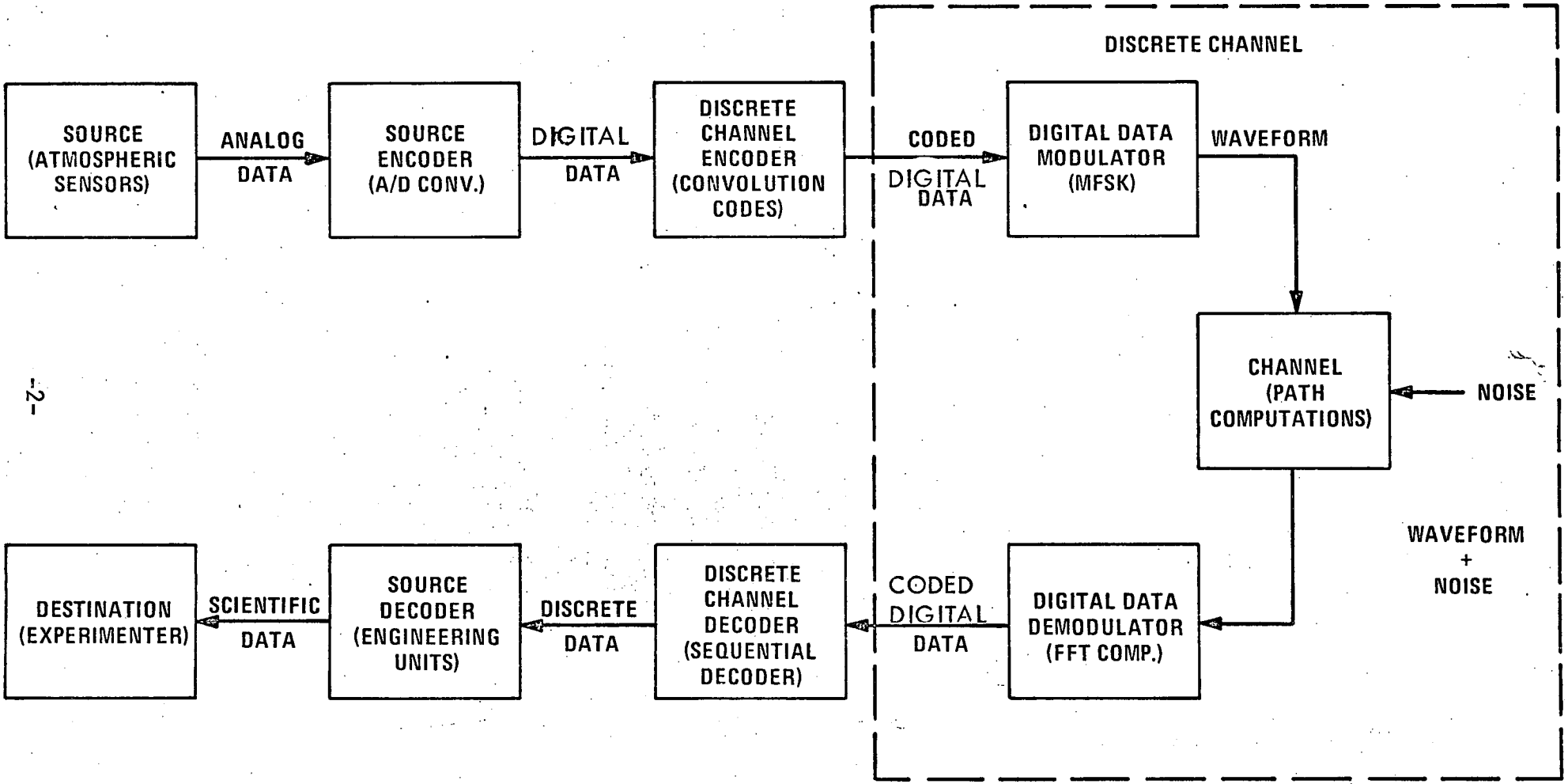

Figure 1.1 BLOCK DIAGRAM OF COMMUNICATIONS SYSTEM

1.2.2 Overall Communications System Channel Model

The class of channel models which we are considering is the class where the set of inputs and outputs are each a set of time functions (waveforms) and for each input waveform the output waveform is a random process. For the initial application, the source, Figure 1.1 is the small probe sensor complement and the source encoder is an A/D converter. When transmitting binary data over a channel in the above class it is convenient to separate the channel encoder and decoder each into two parts. The digital data coming out of the source encoder (A/D converter) enters the discrete channel encoder (for the small probe application a rate $\frac{1}{2}$ convolutional encoder) producing a sequence of symbols from a fixed alphabet, say $a_1, \ldots, a_k$ at fixed time intervals, say one symbol each τ_c seconds. The digital data (for our initial application an MFSK system) produces one of a fixed set of waveforms, say $S_1(t), S_2(t), \ldots S_k(t)$, each of duration τ_c. Thus the entire waveform input to the channel has the form

$$\sum_n S_{i_n}(t-n\tau_c) \tag{1}$$

where the sequence i_n, $n = \ldots -1, 0, 1, \ldots$ is determined by the corresponding inputs to the digital data modulator.

Now this resultant waveform which is input to the channel is attenuated, modified in phase, and Gaussian Noise is added as it passes through the channel. The digital data demodulator takes the received waveform and converts it back to a sequence of symbols from a fixed alphabet. The discrete channel decodes and makes a decision as to what alphabet symbol has been transmitted in the corresponding time interval. In more sophisticated cases the output will also contain information as to how reliable the decision is, yielding an output alphabet of $b_1, \ldots, b_l$. The source decoder and destination are functions of the data itself and will remain unspecified for the purposes of this report.

Since we have framed the overall models in an information theoretic sense we will be able to make use of some standard measures of efficiency for these cases, i.e., channel capacity, noisy channel coding theorem and desired bit rate. Subsequent paragraphs will describe the modelling accomplished to date for the discrete channel portion of the overall model and the utility of these models. Future work will expand upon that discussed here with emphasis upon the portions of Figure 2.2 not yet addressed and upon the output measures of effectiveness.

DISCRETE CHANNEL MODEL

2.1 GENERAL

The mathematical model for the discrete channel which has been developed is partitioned into two major groups, i.e., the input signal generation and the received signal acquisition. The approach taken has been that of establishing a baseline system utilizing the JPL design studies and the GSFC Phase A Explorer Summary Report. This baseline system is being used to insure that the simulation concept is sufficiently flexible to permit detailed tradeoff analyses and that the concept incorporates provisions for growth, as required.

2.2 SIMULATION LOGIC

The gross logic of the simulation as presently envisioned is as follows. Steps a through d are contained in the input signal generator and e through g in the signal acquisition model.

Signal Generation

a. Establish transmitter parameters

b. Compute coded MFSK data set

c. Characterize signal at the receiver as a function of:

   (i) Path loss
   (ii) Random frequency instability
   (iii) Channel fading
   (iv) Channel phase variations

d. Generate random variations on transmitted data set (Gaussian Noise)

Signal Acquisition

e. Generate Fourier coefficients

f. Establish frequency acquisition and synchronization

g. Establish time acquisition and synchronization

Thus, a baseline simulation which has been developed permits the generation of a simulated received signal which incorporates the effects of the transmitter parameters and channel parameters as identified in Table 3.1. The effects of variations in these parameters are assessed by Monte Carlo methods. Increased sophistication in channel models can be accommodated without major modification to the baseline simulation which has been developed.

The signal acquisition model is based upon the work previously accomplished at JPL. It permits the testing of such typical items as decision thresholds for the FFT outputs and acquisition times under various assumptions concerning the input signals and accuracy of the coded signal set.

2.3 GROWTH ITEMS

Growth items for the present baseline simulation include:

a. Encoding and Decoding algorithms;

b. Improved channel characterization;

c. Alternate signal synchronization schemes; and

d. Data window weighting of received signals.

INPUT SIGNAL GENERATION

3.1 GENERAL

The signal which is received at the digital data demodulator can be characterized as a function of the key transmitter parameters, the random disturbances in the channel and the effective noise temperature of the receiving system. The discussion which follows will incorporate into mathematical models the effects of the transmitter and channel key design parameters shown in Table 3.1

3.2 INITIAL COMPUTATIONS

The initial computations which will be made in the simulation are those of received power and nominal signal to noise ratio as follows.[2/]

$$P_R = \frac{P_t G_t}{(4.8\times10^{11})Lf_c^2R^2} \tag{2}$$

$$S/N = \frac{P_t G_t D^2}{(4.9)R^2 T_e W} \tag{3}$$

where P_R = Nominal Received Signal Power (watts)

P_t = Transmitter Power (watts)

G_t = Gain of the Transmitter Antenna (dimensionless)

2/ Low Data Rate Telemetry, Goldstein & Kendal, Proc. of Am. Astron. Soc. Symp. on Unmanned Exploration of the Solar System, February 1965.

TABLE 3.1

KEY DESIGN PARAMETERS

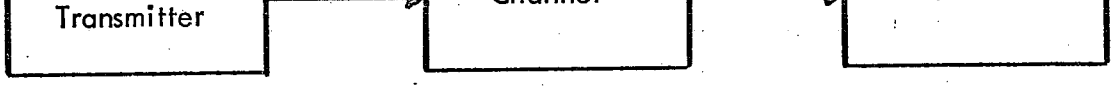

Number of Tones	Planetary Motion (Venus)	Receiver Antenna Gain
Tone Spectral Width (Osc. Thermal noise)	Wind Speed & Turbulence	Receiver Noise Temperature
Time Duration of Tones	Doppler Shift	Signal Detection Method
Coding Method	Atmospheric Effects	Frequency Synchronization Method
Transmitted Power	Gaussian Noise	Time Synchronization Method
Tone Frequency Spacing		Long term Drift Compensation Method
Long Term Drift (Doppler residuals, long term changes, power supply variation)		Doppler Correction
		Oscillator Instability
Carrier Frequency		Decoding Method
Bit Rate		
Antenna Gain		
Bits/Word		
Losses		

L = Losses in the Total System (dimensionless)

f_c = Frequency of the Transmitter Carrier (hertz)

R = Range from Transmitter to Receiver (Astronomical Units)

S/N = Nominal Signal to Noise Power Ratio at the Receiver (dimensionless)

D = Diameter of the Receiving Antenna (meters)

T_e = System Effective Noise Temperature (degrees kelvin)

W = System Bandwidth (hertz)

3.3 INTRODUCTION OF RANDOM VARIATIONS

Having established nominal values for transmitted power and signal/noise power ratio at the receiver, it is necessary to introduce the effects of random variations in the transmitter and channel parameters. After carrier demodulation the received signal will be assumed to be of the form:

$$X(t) = A \cos (2\pi f_r t + \phi) + n(t) \tag{4}$$

where: A = Amplitude of the Received Signal

f_r = the signalling frequency plus frequency error

ϕ = unknown phase term

$n(t)$ = random noise process

In order to model the effects of the random variations we will use a Monte Carlo process in which probability distributions will be established for the random variables of interest. Random samples will then be drawn from these probability distributions for each of the random variables at times coinciding with the sampling rate of the system. These random samples will be added to the nominal values of the received signal in order to establish stochastic variations in the signal at each sampling interval.

Mathematically,

$$X(t_i) = S(t_i) + N(t_i) \tag{5}$$

$$S(t_i) = \sqrt{2(P_R + \triangle P_{R_i})} \cos \left[2\pi f_K t_i + \triangle \phi_i + \triangle \theta_i \right] \tag{6}$$

$$N(t_i) = \left[\sqrt{2(P_R + \triangle P_{R_i})} \right] \cos (\triangle \alpha) \tag{7}$$

where: $S(t_i)$ = Received Signal at Time t_i

$N(t_i)$ = Noise Signal at Time t_i

ΔP_{R_i} = Random Sample of Signal Amplitude Variation at Time t_i

f_K = Signalling Frequency

$\Delta \phi_i$ = Random Sample of Phase Variation due to Long Term Drift at Time t_i

$\Delta \theta_i$ = Random Sample of Phase Variation Due to Short Term Drift at Time t_i

$\Delta \alpha$ = Random Sample of Phase Variation Due to Channel Noise at time t_i

Thus utilizing equations (2), (3), (5), (6) and (7) we have modelled the received signal in terms of the key design parameters for the transmitter and the channel shown in Table 3.1. Figure 3.1 presents a flow chart of the method by which the composite input signal for a specified time period will be computed in the software routine. Appendix A presents a discussion of the sampling routine which is being utilized and the probability distributions which are available for sampling purposes.

In Figure 3.1 we start by setting the K counter equal to 1. This counter represents the number of frequency bands which are stepped through during the receive signal acquisition process. Details of this process are discussed later in this report. Next the counter i is set to zero. This counter represents the total number of samples (N) to be taken over the specified time period for the simulation run. In order that no information be lost due to the sampling interval the number of samples must satisfy

$$N \geq 2T_B W \tag{8}$$

where T_B = Signalling Interval (Sec.)

W = Receiver Bandwidth (Hz)

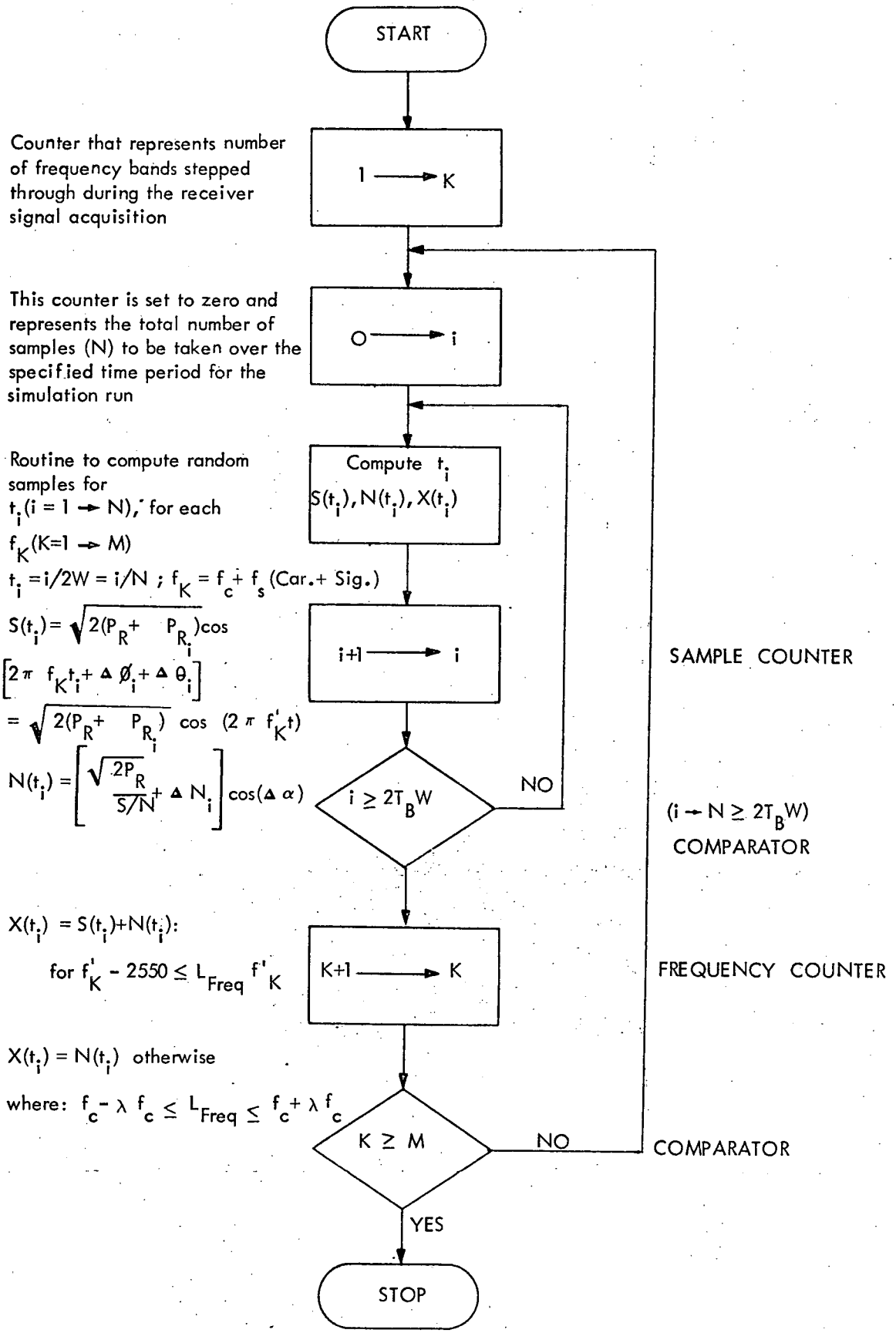

Figure 3.1 INPUT SIGNAL GENERATOR

SIGNAL ACQUISITION MODEL

4.1 GENERAL

For the MFSK system under consideration we must synchronize the signal in both time and frequency, where time synthronization is defined as the correct timing between the transmitter and receiver at the beginning of each transmitted word and frequency synchronization is defined as the correct location at the receiver of the position of the carrier frequency in the spectrum. Figure 4.1 illustrates a basic MFSK receiver. The receiver bases its decision upon an estimated Fourier power spectrum of the received input. It is assumed that an acquisition sequence of two alternating frequencies is transmitted prior to initiation of data transmission.

4.2 FREQUENCY ACQUISITION AND TRACKING[3/]

Equation (4) previously described the form of the received signal after carrier demodulation and will be repeated here

$$X(t) = A \cos (2\pi f_r t + \emptyset) + n(t) \tag{4}$$

Using a discrete Fourier transform[4/] to obtain the power spectrum of the received signal we calculate the Fourier coefficients

$$r_k = (a_k^2 + b_k^2)^{1/2} \tag{9}$$

$$a_k = \sum_{i=0}^{N-1} X_i \operatorname{Cos} \left(2\pi \frac{ik}{N}\right) \qquad k = 0, 1, 2\ldots, N/2 \tag{10}$$

3/ This discussion is drawn from JPL Space Programs Summary 37-52 and 37-57, Vol III

4/ Appendix B presents additional detail concerning the discrete Fourier Transform

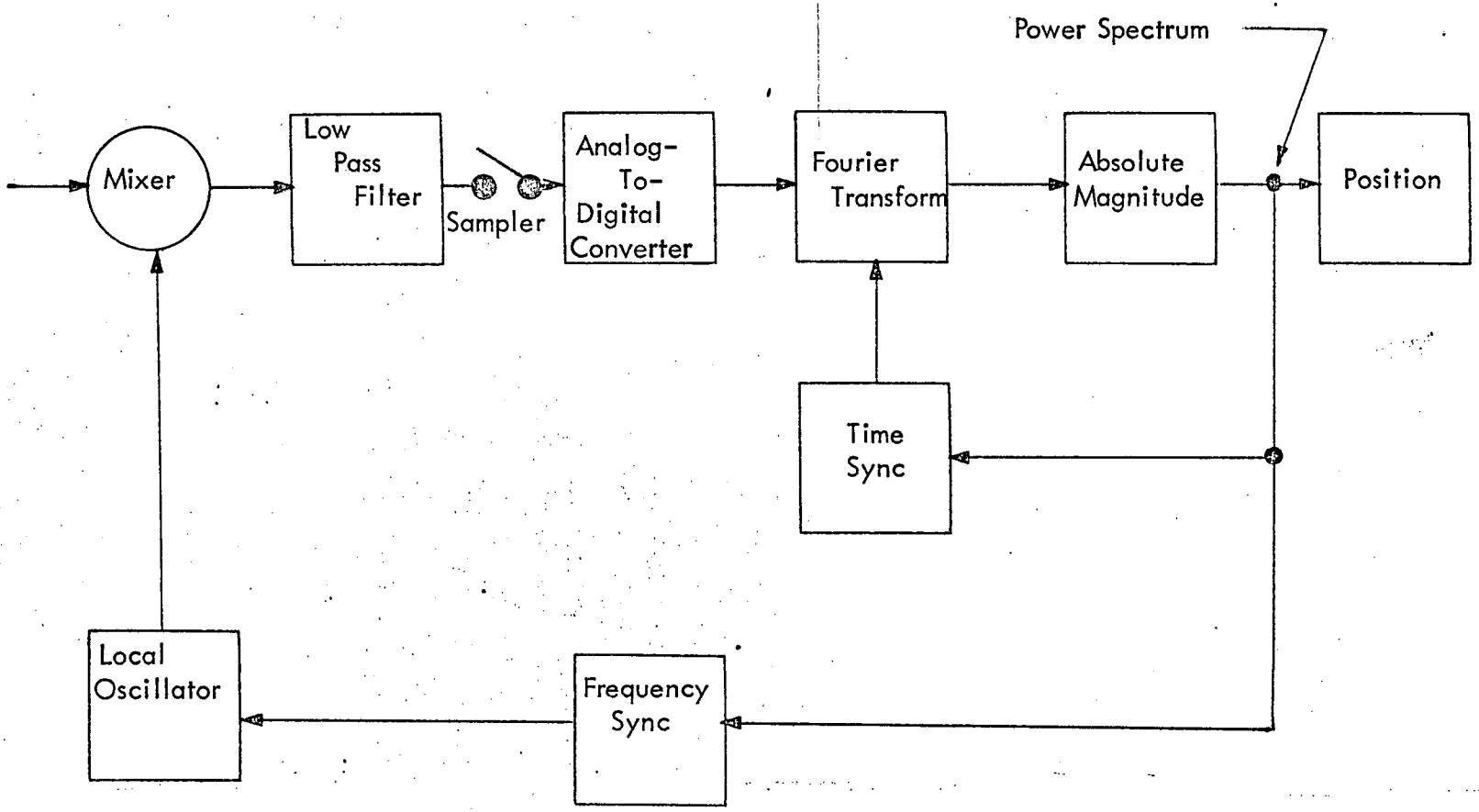

Figure 4.1 MSFK RECEIVER BLOCK DIAGRAM

$$b_k = \sum_{i=0}^{N-1} X_i \sin\left(2\pi \frac{ik}{N}\right) \qquad k = 0, 1, 2\ldots, N/2 \tag{11}$$

where $X_i = X(\frac{iT}{N})$ are the sampled values of X(t).

The values of T & N are chosen with reference to the sampling theorem. If at least N samples are taken during the interval T (N = 2WT) where the process is low pass filtered to a bandwidth W and sampled at a rate 2W; then no information has been lost about the sampled waveform.

Due to instabilities in the transmitter and receiver oscillators and to uncompensated doppler shifts, it is not possible to know in advance the carrier frequency which will be received at the receiver. The actual received carrier frequency (f_c) may be represented by $f_c + \lambda f_c$ where λ is a factor representing the difference between the actual and the nominal carrier frequencies.

This initial frequency error is usually much larger than the bandwidth W of the Fourier spectrum process. However, an upper bound can be put on this initial error by a knowledge of the maximum anticipated doppler frequency shifts and by a knowledge of the long and short term oscillator drifts. This upper bound is say $K_{max}W$ such that

$$-K_{max}W \leq f_c \leq K_{max}W \tag{12}$$

If the local oscillator is stepped in frequency from $f_c - K_{max}W$ to $f_c + K_{max}W$, in steps of W and the spectrum is computed in each band over a 2T second interval we can look for peaks in the band which exceed a threshold and use these peaks as a decision criteria for whether or not a signal is present. This is the procedure which is used in frequency acquisition.

In order to track the frequency, we require an estimate of the frequency error. The estimator must be a function of the Fourier spectral components r_k. One approximation to a maximum likelihood estimator of the true frequency used in this initial simulation is as follows. Other estimates are possible and should be tested.[5/]

$$\hat{\varsigma} = \frac{r_{+1} - r_{-1}}{r_{+1} + r_{-1}} \tag{13}$$

where $\hat{\varsigma}$ = maximum likelihood estimator at true Fourier frequency component

r_{+1} = magnitude of the Fourier frequency component higher than the present estimate

r_{-1} = magnitude of the Fourier frequency component lower than the present estimate

---

5/ "Frequency Tracking in An MFSK Receiver", by H. D. Chadwick, JPL Report #900-268, April 30, 1969.

This estimator can be used to design the frequency tracking loop. A general form of this loop is shown by Figure 4.2a. The estimator block output $\hat{\varsigma}$ is defined as follows:

$$\hat{\varsigma} = E(\hat{s}) + N_\varsigma = g(s) + N_\varsigma$$

where: $g(s) = E(\hat{s})$ is the nonlinear operation on the time error ς produced by the estimator.

N_ς = is the additional noise term.

Figure 4.2a can then be rewritten as shown by Figure 4.2b. Substituting $F(S) = SH(s)$ Figure 4.2b becomes Figure 4.2c. It is seen that this is equivalent to the standard block diagram of a phase-lock loop with nonlinearity $g(s)$ replacing that of the phase detector. A second-order loop can be synthesized and because of the highly nonlinear nature of the function $g(s)$ the theoretical performance of the loop can be calculated by

- The use of nonlinear approximation to the nonlinearity $g(s)$ with the standard linear phase-lock loop approximation.
- non-linear phase-lock loop analysis

The values of the variance of the frequency error, for the linear approximation and non-linear methods respectively are desired for comparative purposes.

The tracking loop must convert the $\hat{\varsigma}$ estimator into an estimate of frequency error Δf. An actual MFSK receiver updates its estimate of the frequency error once every T seconds, requiring that the error remain small between these discrete sampling times. Three different discrete equivalent tracking loop filters for simulation purposes are shown by Figure 4.3. A loop simulation program can be implemented on a digital computer using Monte Carlo techniques to test each of the equivalent tracking loop filters. The objective is to obtain an interpolated error function (Δf) at a rate ten times faster than the calculation of the estimate. From the results, that version offering the best solution, will be implemented in the overall MFSK simulation program.

4.3 TIME SYNCHRONIZATION[6/]

Again assuming a receiver bandwidth of W and sampling at or above the Nyquist rate as in equation (8) then if the receiver is not time synchronized with the transmitter, then the N samples will overlap two frequencies. Figure 4.4 illustrates the case. Note that as previously we are assuming an acquisition sequence of two alternating frequencies (f_1 & f_2) is transmitted prior to data transmission. As seen in Figure 4.4, we have n samples from f_1 and (N-n) samples from f_2.

6/ Drawn from: "Time Synchronization in an MFSK Receiver", by H.D. Chadwick, JPL Space Programs Summary 37-48, Vol III.

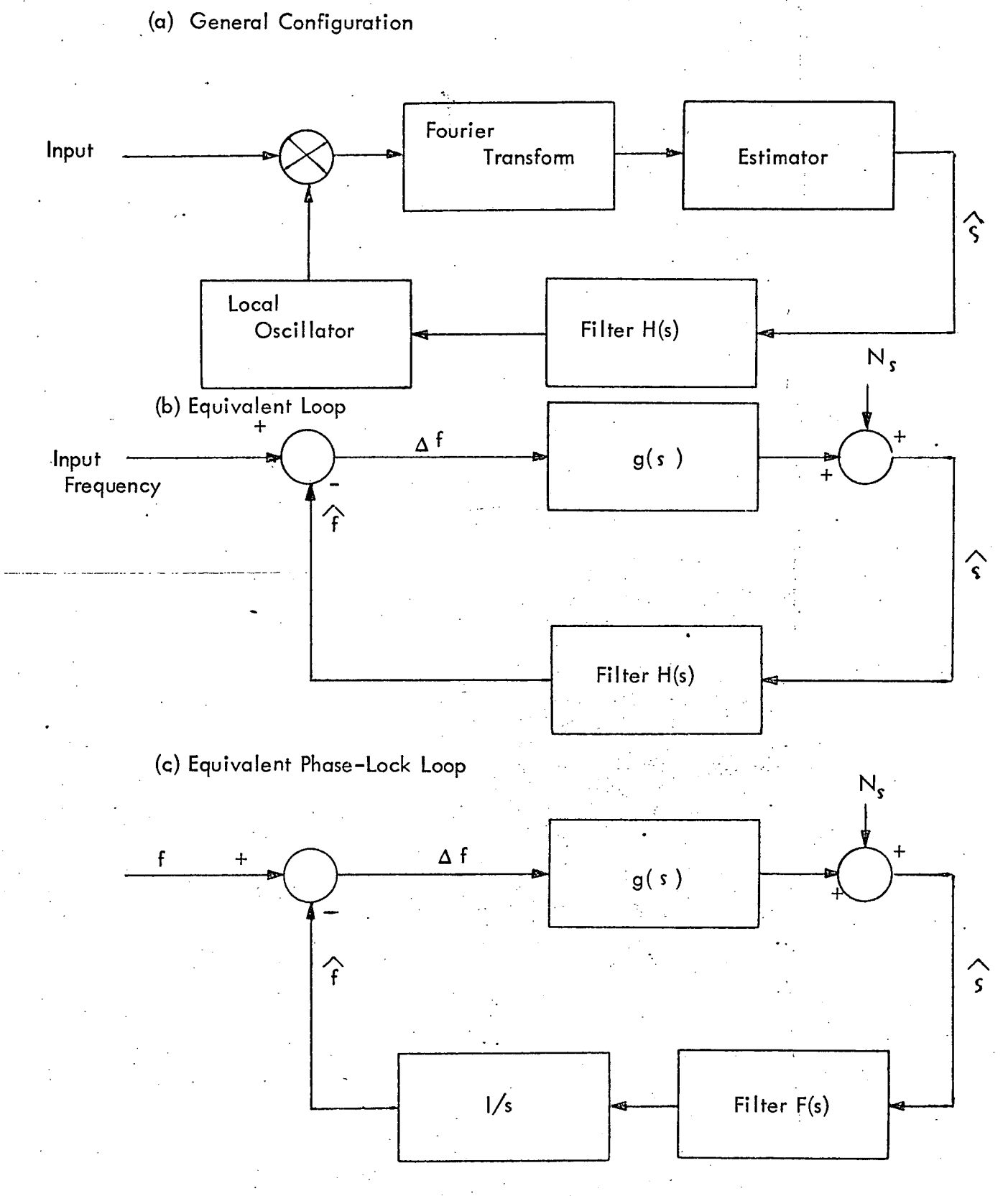

Figure 4.2 FREQUENCY TRACKING LOOP

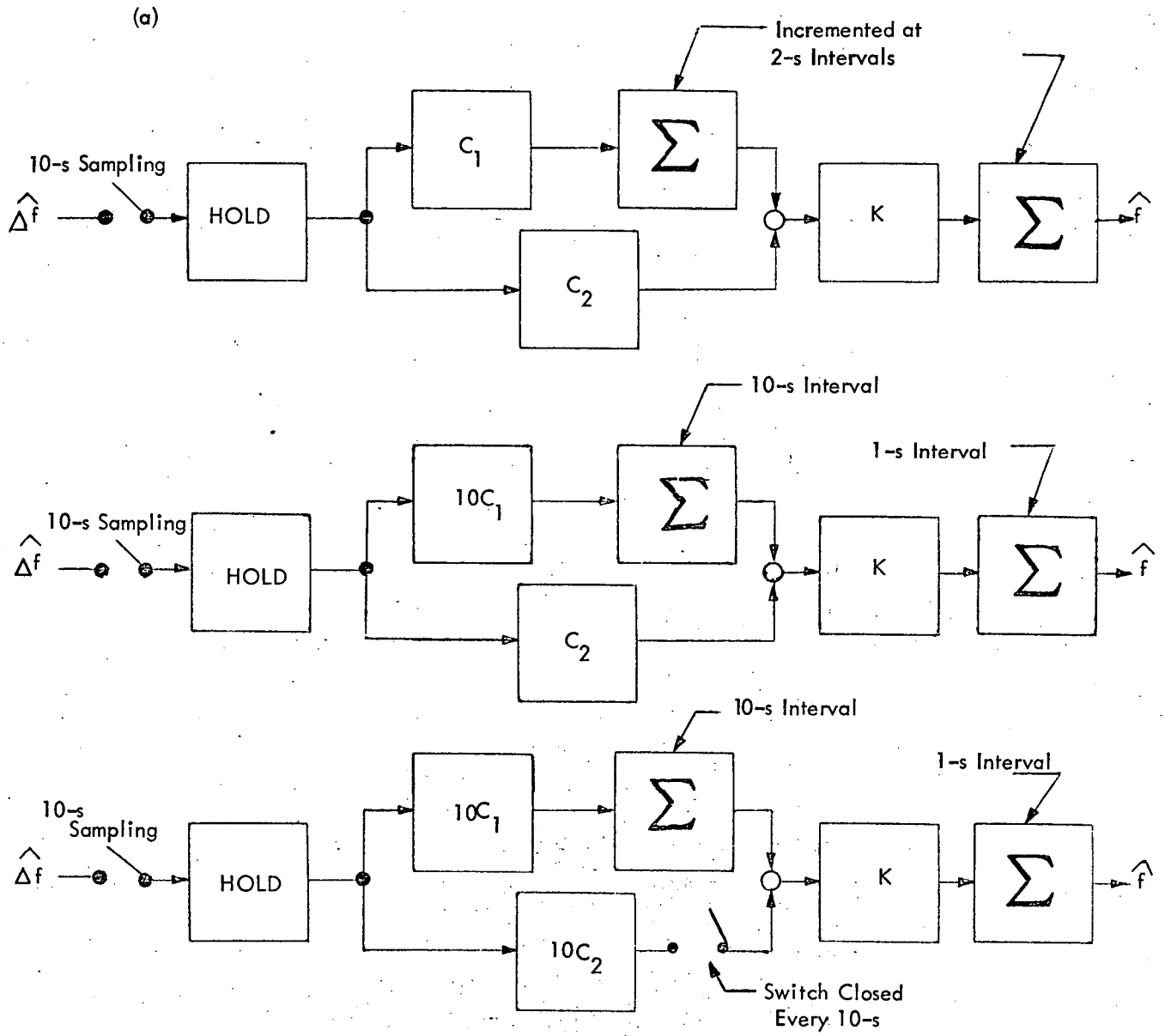

Figure 4.3 THREE VERSIONS OF DISCRETE EQUIVALENT TO FILTER H(s)

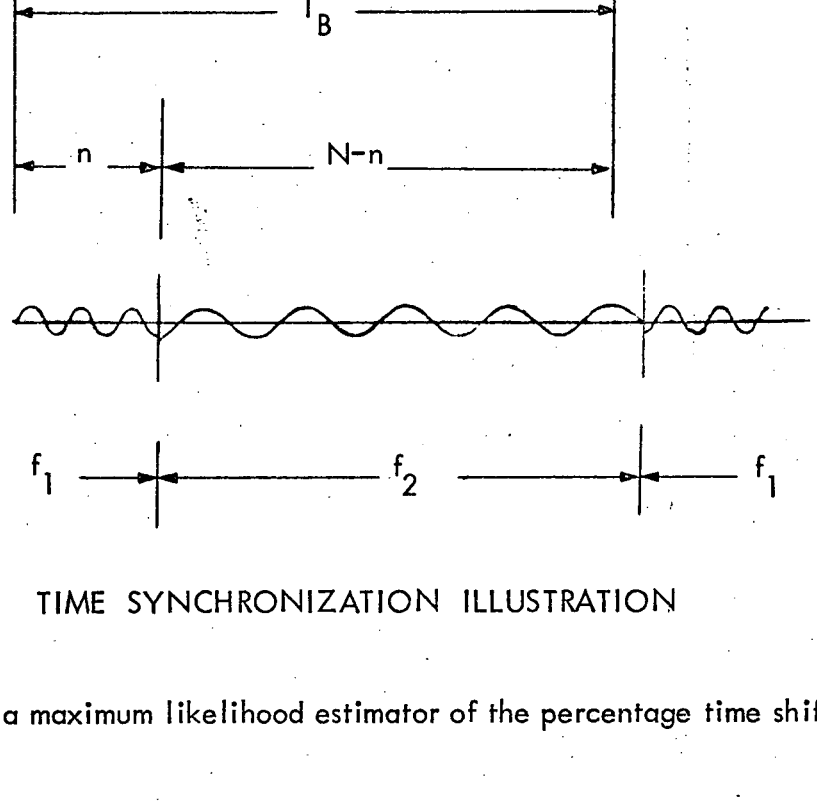

Figure 4.4 TIME SYNCHRONIZATION ILLUSTRATION

It has been shown[7/] that a maximum likelihood estimator of the percentage time shift (E) is given by

$$\hat{\epsilon} = \frac{r_2 - r_1}{2(r_1 + r_2)} \tag{15}$$

where r_1 & r_2 are the Fourier coefficients from the FFT output.

Figure 4.5 gives a block diagram of a closed loop time synchronization technique which can be simulated by digital techniques.

4.4 PREVIOUSLY DEVELOPED SIMULATION MODEL

JPL has programmed the equations presented above. Figure 4.6 presents an overall flowchart of the program and Figures 4.7 to 4.12 present one more level of breakdown for Figure 4.6. Work is underway to convert and modify this program for use on the Interdata machine. Appendix C presents detailed flowcharts of the pertinent sub-programs included in Figures 4.6 to 4.12.

7/ ibid

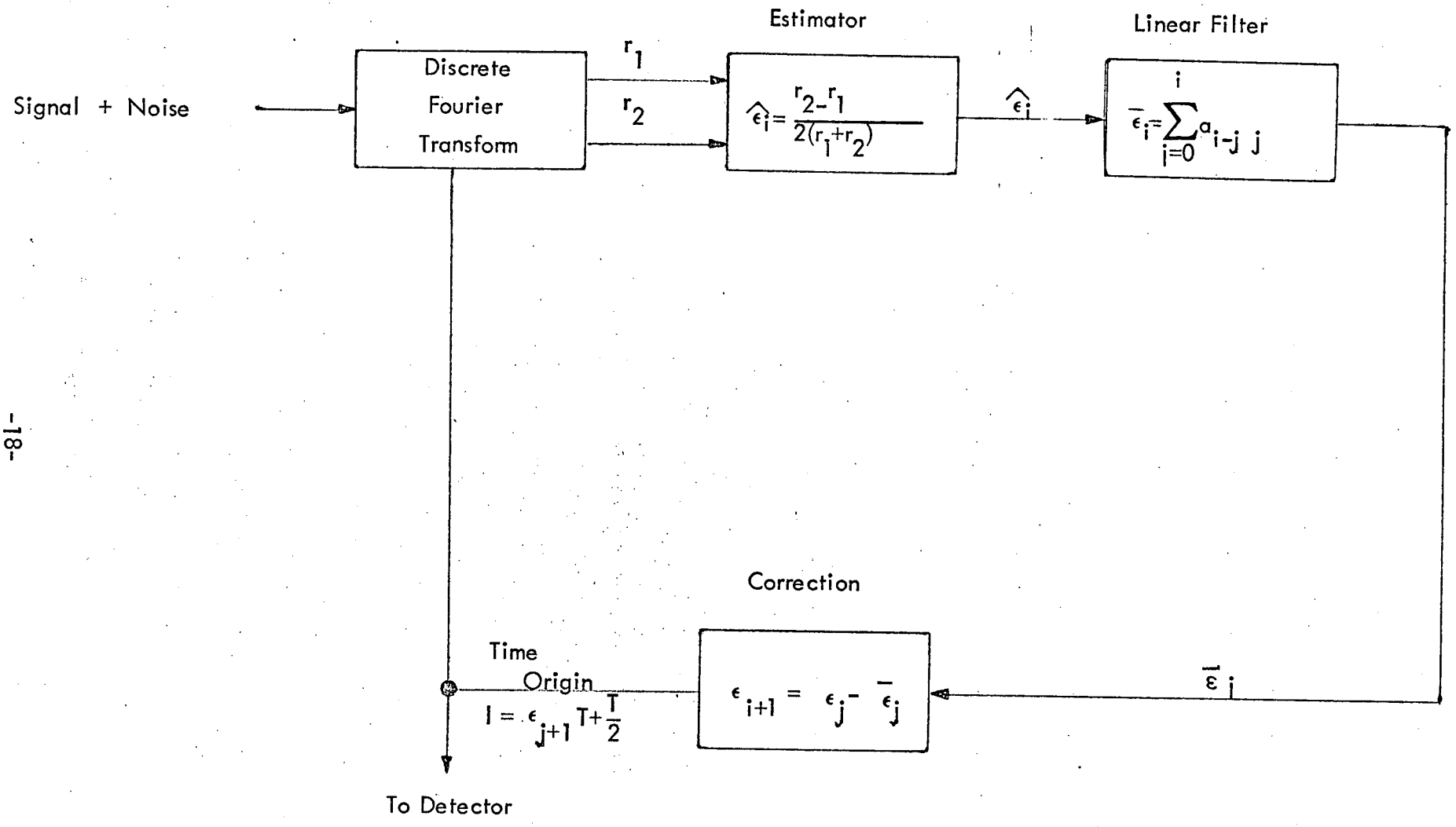

Figure 4.5 BLOCK DIAGRAM OF CLOSED-LOOP SYNCHRONIZATION TECHNIQUE

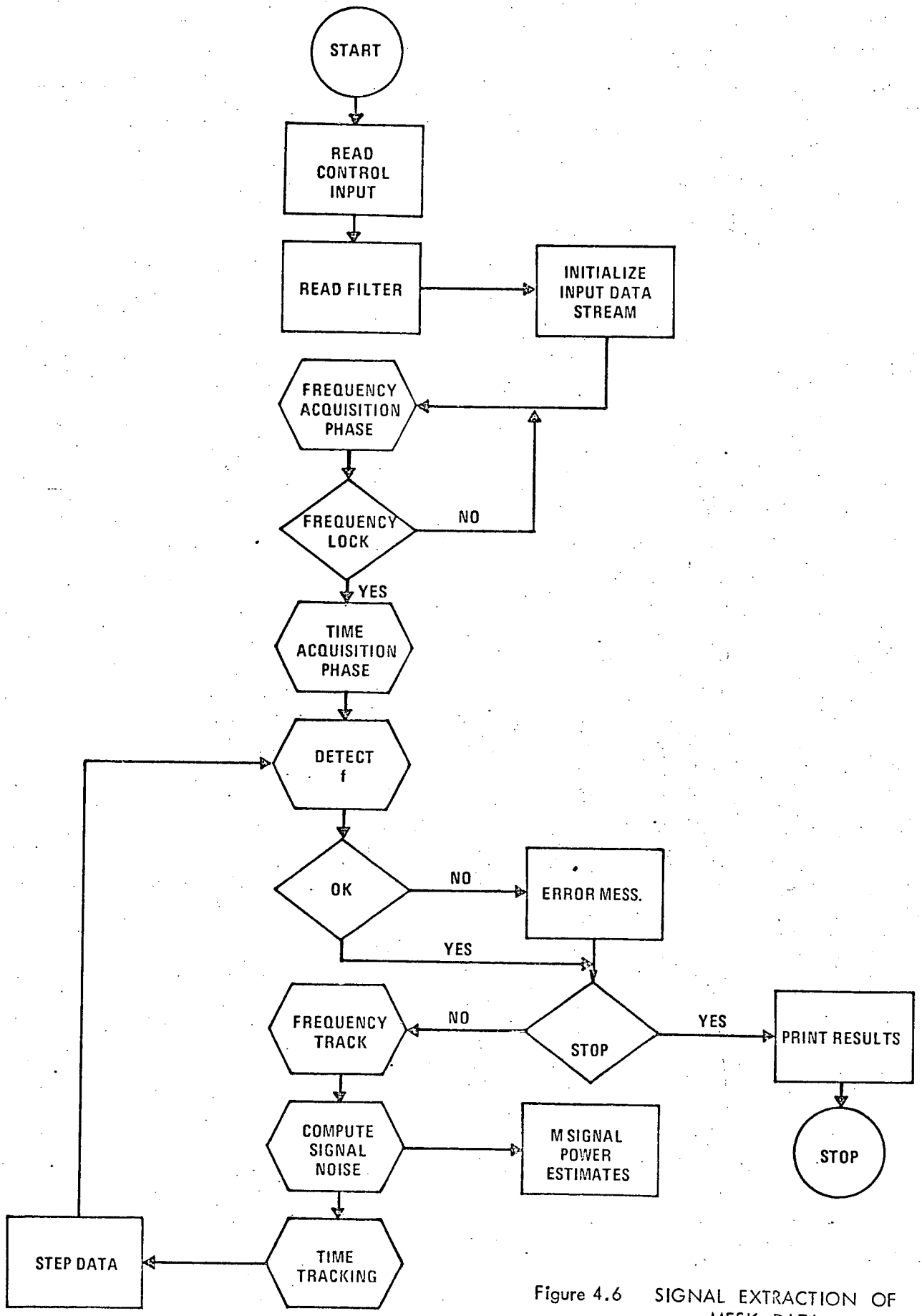

Figure 4.6 SIGNAL EXTRACTION OF MFSK DATA

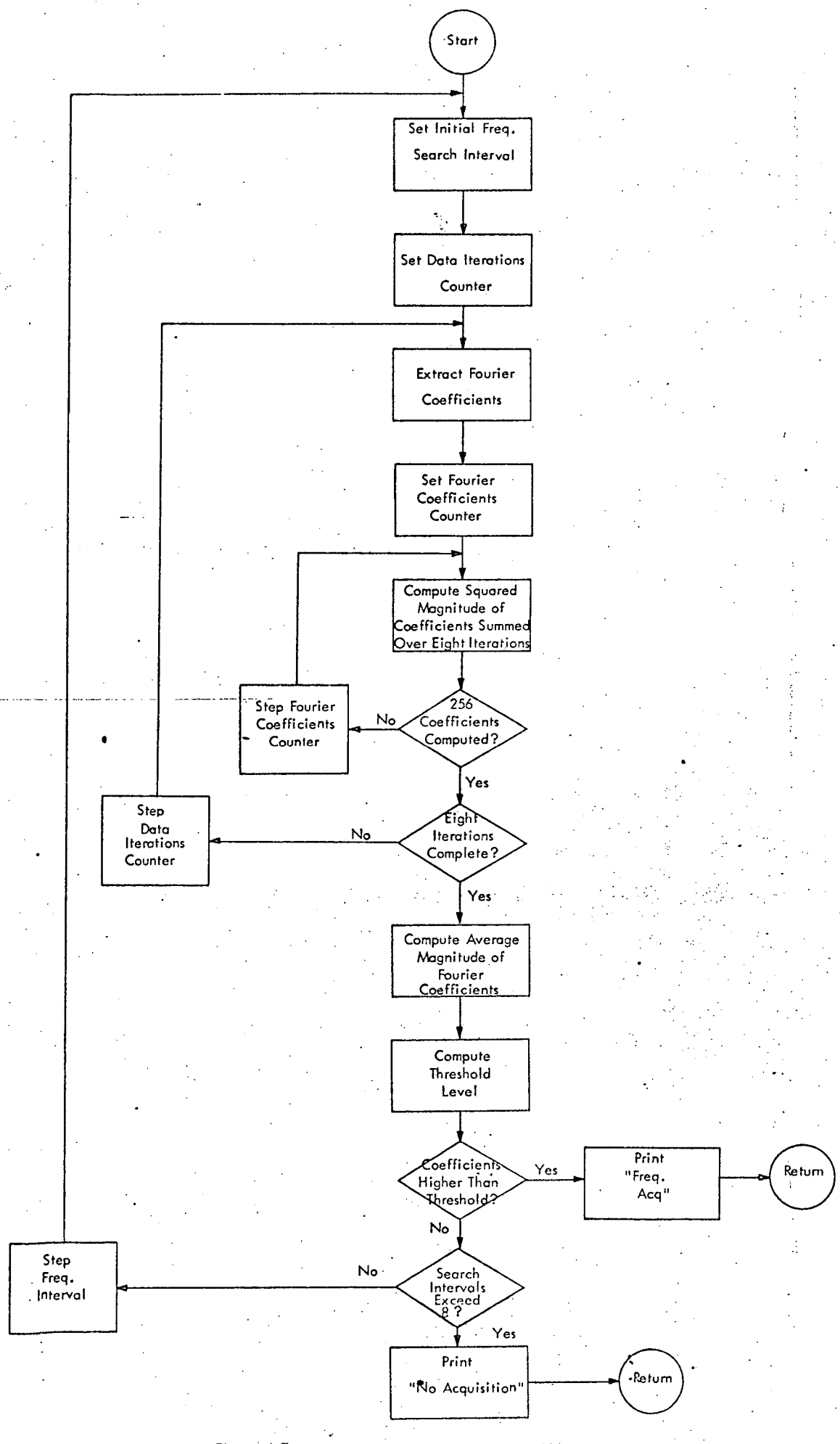

Figure 4.7 FREQUENCY ACQUISITION

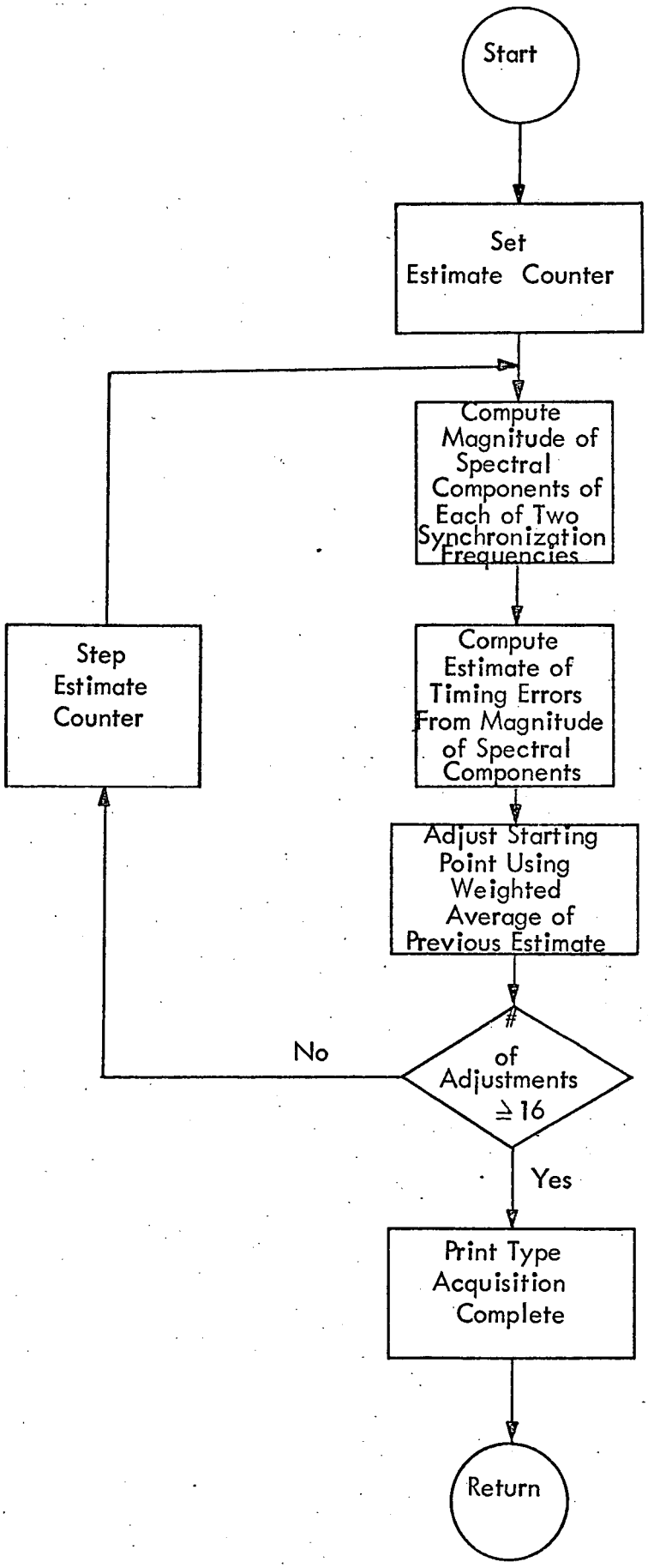

Figure 4.8 . TIME ACQUISITION (See Figure 4.5)

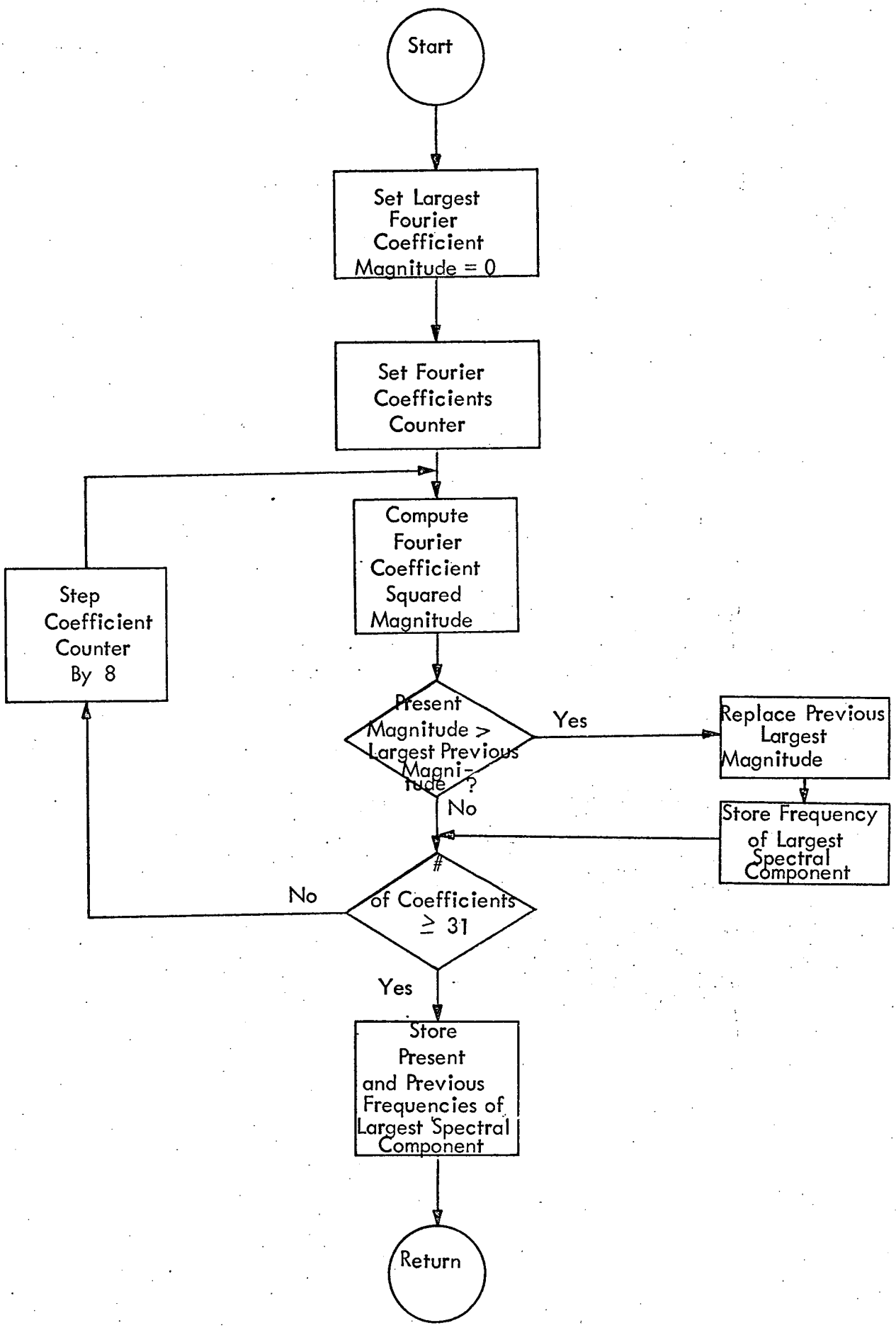

Figure 4.9 DETECT

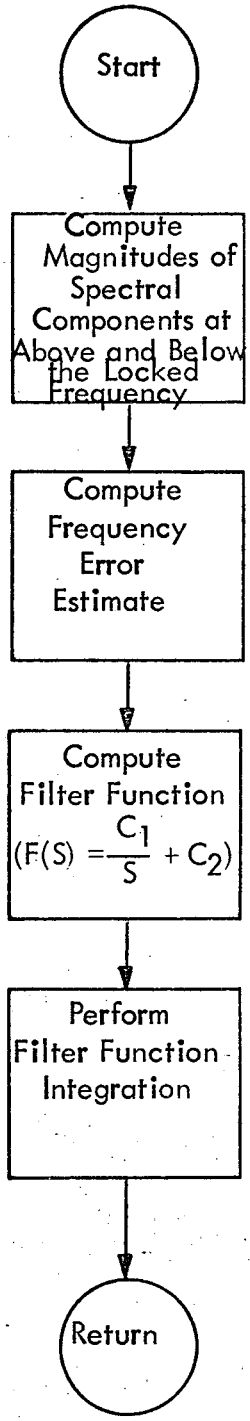

Figure 4.10 FREQUENCY TRACKING AND INTEGRATION
(See Figure 4.2C, Equivalent Phase Lock Loop)

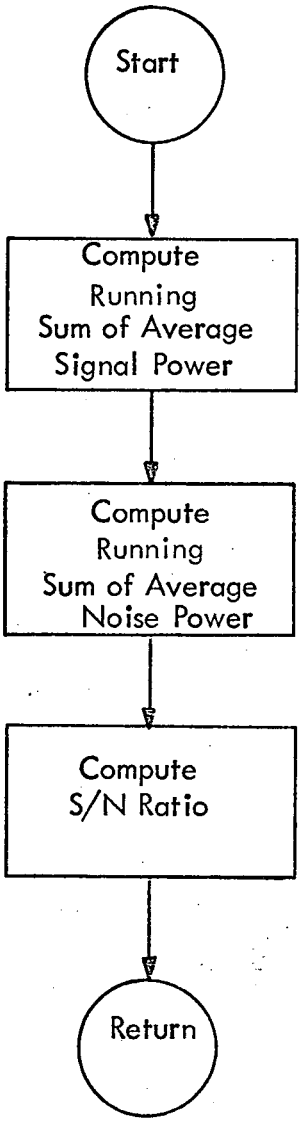

Figure 4.11 S/N ESTIMATE

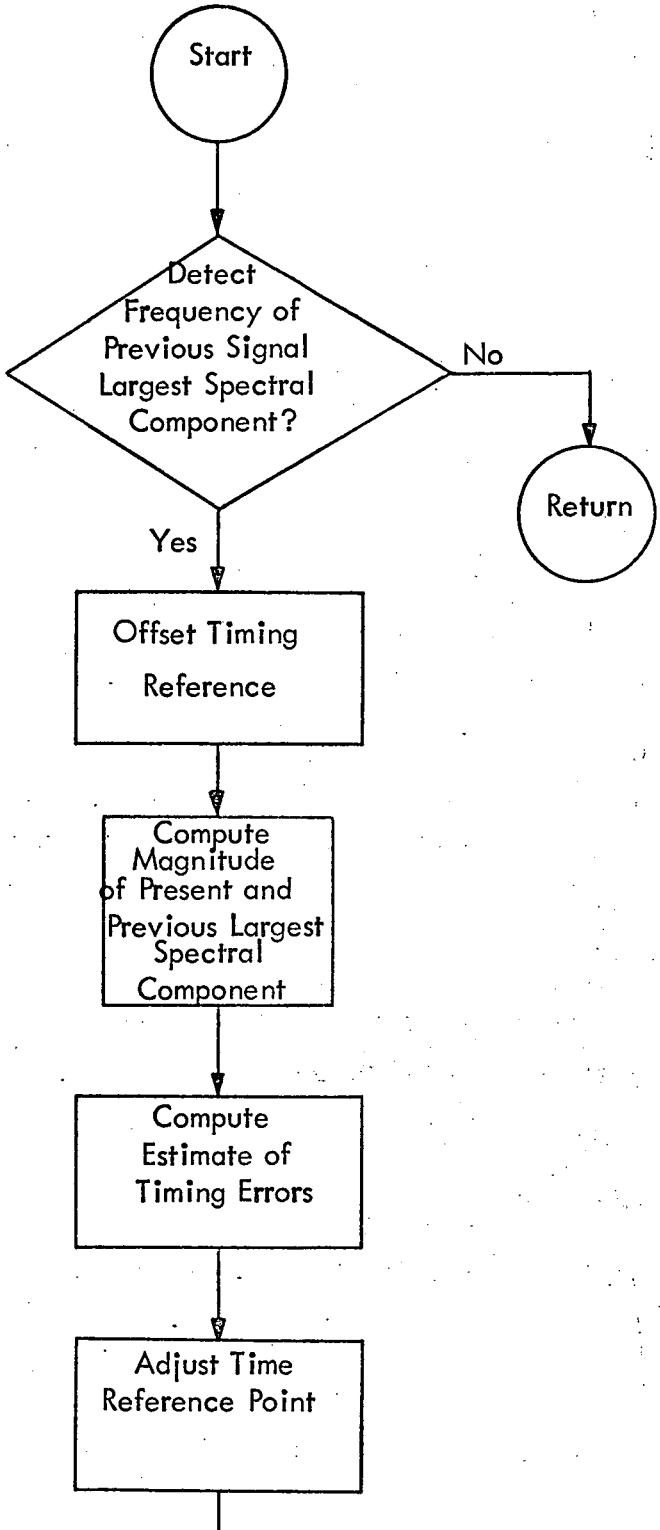

Figure 4.12 TIME SYNCHRONIZATION TRACKING

APPENDIX A

DISCRETE FOURIER TRANSFORM CONSIDERATIONS

DISCRETE FOURIER TRANSFORM CONSIDERATIONS[A.1/]

The Fourier transform has long been used for characterizing linear systems and for identifying the frequency components making up a continuous waveform. However, when the waveform is sampled, or the system is to be analyzed on a digital computer, it is the finite, discrete version of the fourier transform (DFT) that must be understood and used. The fast Fourier transform (FFT) is simply an efficient method for computing the DFT. The FFT can be used in place of the continuous Fourier transform only to the extent that the DFT could before, but with a substantial reduction in computer time.

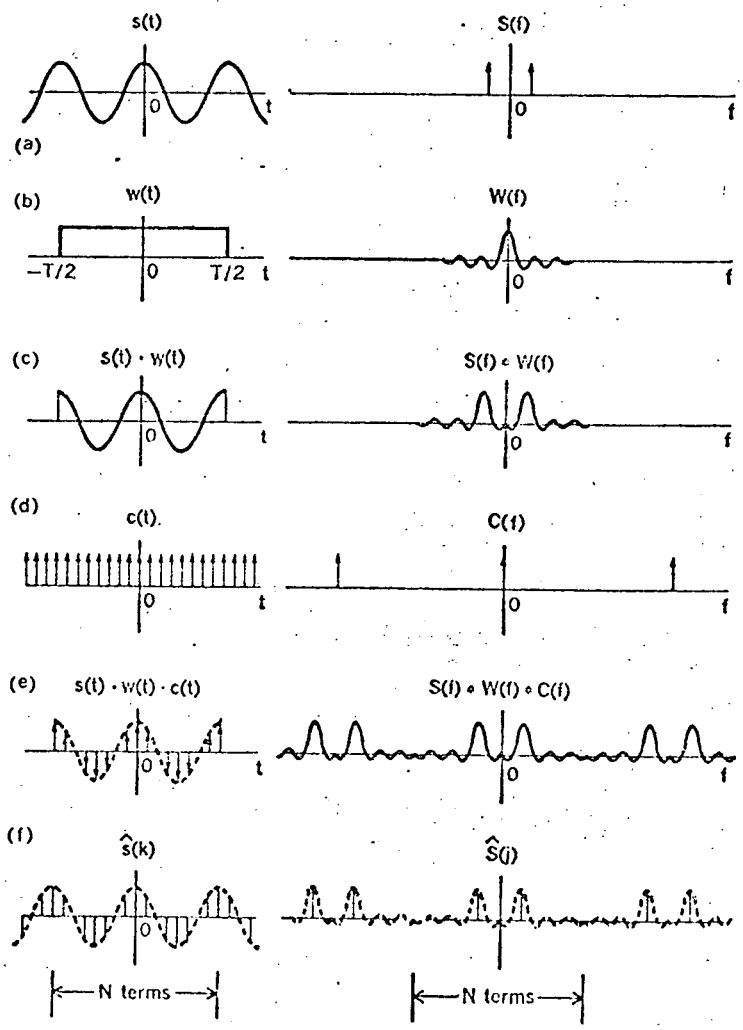

Figure A.1 Discrete Versus Continuous Fourier Transform

A.1/ Drawn from: "A Guided Tour of the Fast Fourier Transform" by G. Bergland, IEEE Spectrum, July 1969.

"The Measurement of Power Spectra", by Blackman & Tukey, Dover Publications, 1958

Consulting Figure A.1 we illustrate the differences between the discrete and continuous transforms. Line (a) represents the continuous Fourier transform of S(t), a cosine wave. W(t) in line (b) represents a finite time window and its continuous transform through which we obtain samples of the signal. The portion of S(t) to be analyzed from the sampled data is shown in line (c) as the product of S(t) and W(t) in the time domain and as their corresponding convolution in the frequency domain. Lines (d) and (e) show the digital sampling operations and the resulting transforms. The continuous frequency domain function shown in line (e) can be made discrete if the time function is treated as one period of a periodic function (line (f)). Thus the DFT is simply a reversible mapping of N terms of $\hat{S}(k)$ into N terms of $\hat{S}(j)$.

The three problems most often encountered in using the discrete Fourier transform appear to be aliasing, leakage, and the picket-fence effect. The term "aliasing" refers to the fact that high-frequency components of a time function can be impersonated by low frequencies if the sampling rate is too low. This uncertainty can be removed by demanding that the sampling rate be high enough for the highest frequency present to be sampled at least twice during each cycle.

The "leakage" problem is associated with the effects of the rectangular data window shown in Figure A.1 line (b) resulting in a frequency domain function with an amplitude of the $\frac{\sin x}{x}$ form. The sidelobes of this function represent leakage into frequencies other than the true frequency.

The "picket fence" effect is caused by the cumulative effect of the $\frac{\sin x}{x}$ spreading of each Fourier coefficient. Thus instead of a line spectrum for each coefficient term we observe the phenomena shown in Figure A.2

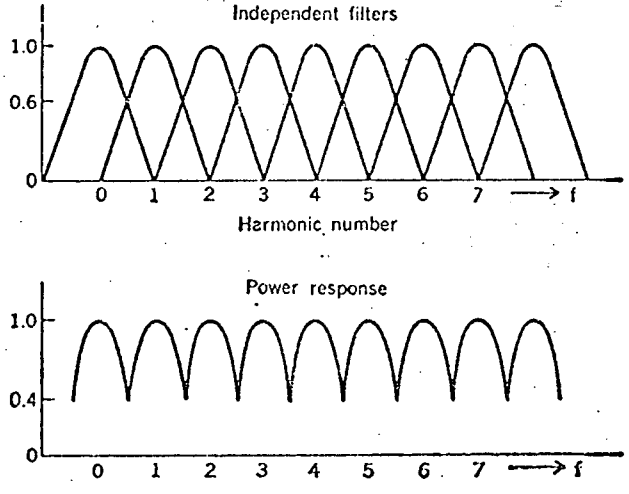

Figure A.2 The Response of the Discrete Fourier and Transform Fourier Coefficients Viewed as a Set of Bandpass Filters (Picket-Fence Effect).

APPENDIX B

GENERALIZED RANDOM VARIABLE GENERATOR

PURPOSE

The CURL subroutine may be used to generate random variables from several different standard distributions in addition to arbitrary, by inverse cumulative distribution curves read by the RDCUR subroutine.

CURL

The CURL routine is called by using '...CURL (ICV, P1, @2...' in an arithmetic expression where ICV, P1 and P2 are described in detail in Table B.1

The RNG routine is used by CURL to generate a uniform random number, N, between 0. and 1. This random number is then used as the argument for an inverse cumulative probability distribution which may be formally evaluated or given in the linear curve format specified for the YLIN subroutine. The YLIN routine is used by CURL to evaluate the arbitrary curves.

The distributions currently allowed in CURL are as follows:

ICV	Distribution
> 0	Arbitrary inverse cumulative probability linear curve [ICV]
0	Constant
-1	Exponential
-2	Bernoulli
-3	Weibull
-4	Extreme value
-5	Normal
-6	Log normal
-7	Uniform
-8	Beta

TABLE B.1

CURL PROBABILITY LAWS AND DISTRIBUTIONS

t = Random variable put into CURL before exit

N = Random variable between 0 and 1

ICV	Name	P_1	P_2	Definition	Computation
> 0	Arbitrary	Scale Factor	Minimum Value	$F_T(\tau)$ = Probability $[t \leq \tau], 0 \leq \tau \leq 1$ = 0 elsewhere where F_T is any arbirtrary cumulative distribution function truncated and normalized so that $0 \leq \tau \leq 1$. Each F_T is defined and assigned a number > 0 on input	$t = P_1 F_T^{-1}(N) + P_2$ F_T^{-1} is the curve read by RDCUR
0	Constant	t_o = Constant	0	$f(t_o) = 1, 0 \leq t_o < \infty$ = 0 elsewhere i.e., constant value t_o is always selected	$t = P_1 + P_2$
-1	Exponential	Mean Value $P_1 > 0$	0	$f(t) = \frac{e^{-\frac{t}{P_1}}}{P_1}$ $t > 0$ = 0 elsewhere	$t = -P_1 \ln(N)$
-2	Bernoulli	p(e) = probability of error $0 \leq P(e) \leq 1$	0	$f(t) = p(e), t = 1$ $= 1 - p(e), t = 0$ = 0 elsewhere	$N > P_1, t = 0$ (never) $N < P_1, t = 1$ (now)

CURL PROBABILITY LAWS AND DISTRIBUTIONS (Cont)

ICV	Name	P_1	P_2	Definition	Computation
-3	Weibull	Location parameter, $P_1 > 0$	Shape parameter, $P_2 > 0$	$f(t) = \frac{P_2}{P_1} t^{(P_2 - 1)} \exp[-\frac{t}{P_1}]$, $t > 0$ $= 0$ elsewhere	$t = [-P_1 \ln N]^{\frac{1}{P_2}}$
-4	Extreme value of the first asymptote	$P_1 \neq 0$		$f(t) = \frac{\exp}{P_1}\left[\frac{-1}{P_1}(t - P_2) - \exp[\frac{-1}{P_1}(t - P_2)]\right]$, $t > 0$ $= 0$ elsewhere	$t = P_1 \ln[-\ln N] + P_2$
-5	Normal	Standard deviation, $P_1 > 0$	Mean value	$\Phi_T(t) = \int_{-\infty}^{\frac{t - P_2}{P_1}} \frac{1}{\sqrt{2\pi}} \exp[-\frac{t^2}{2}] dt$, $t > 0$ $= 0$ elsewhere	$t = P_1 \Phi_T^{-1}(N) + P_2$
-6	Log Normal	$P_1 > 0$ Standard deviation of ln t	Mean value of ln t	$\Phi_{\ln T}(t) = \Phi_T(\ln t)$ $t > 0$ $= 0$ elsewhere	$t = \exp[P_1 \Phi_{\ln T}^{-1}(N) + P_2]$
-7	Uniform	Minimum value	Maximum value	$f(t) = \frac{1}{P_2 - P_1}$ $P_1 < t < P_2$ $= 0$ elsewhere	$t = P_1 + (P_2 - P_1) N$
-8	Beta	$a > 1$	$b > 1$	$f(t) = \frac{\Gamma(a + b)}{\Gamma(a)\Gamma(b)} t^a (1-t)^b$ $0 < t < 1$ $= 0$ elsewhere	See page 945-26.5.22 of NBS Handbook of Math Functions

RDCUR

The RDCUR routine may be used to read in any inverse cumulative probability linear curves which are to be used by CURL in the run. When RDCUR is called, the following data are read from unit 5.

Card	Columns	Description
1	1-10	NCUR, number of arbitrary inverse cumulative density curves (≥ 0). If NCUR>0, the following cards are read for each curve:
2	1-10	NPTS, the number of points in this linear curve
3	6-10 col. fields	The coordinates of the curve points consisting of the probability, followed by the value of 5, in non-decreasing order of probability. (3 points per card).

Repeat card 3 as needed.

Repeat cards 2 and 3 as needed.

The above input data if NCUR is greater than zero must be stored in the following COMMON variable locations which are accessible to the CURL routine.

NCUR....., holds the number of arbitrary curves

CURL ( )... dimensioned sufficiently to hold the tables

LOCCUR ( ). dimensioned at least NCUR.

Subroutine used by CURL

RNG
YLIN
XNORD

APPENDIX C

SIGNAL EXTRACTION FLOW CHARTS

APPENDIX C - SIGNAL EXTRACTION FLOW CHARTS

The flow charts contained in this appendix were developed by analysis of the program listings for the JPL simulation of the MFSK low bit rate receiver. Neither program documentation or program flow charts were available other than the listings.

The contract requires that the JPL simulation be utilized on the Interdata machine as a portion of the baseline simulation being developed. Thus, analysis of the program listings and development of detailed flow charts is a necessary first step in understanding what was simulated and in converting the JPL programs written in both FORTRAN and machine language to the language used on the Interdata machine. The mathematical description of the time and frequency synchronization operations (described in the main body of the report) were also utilized in developing an understanding of JPL program listings.

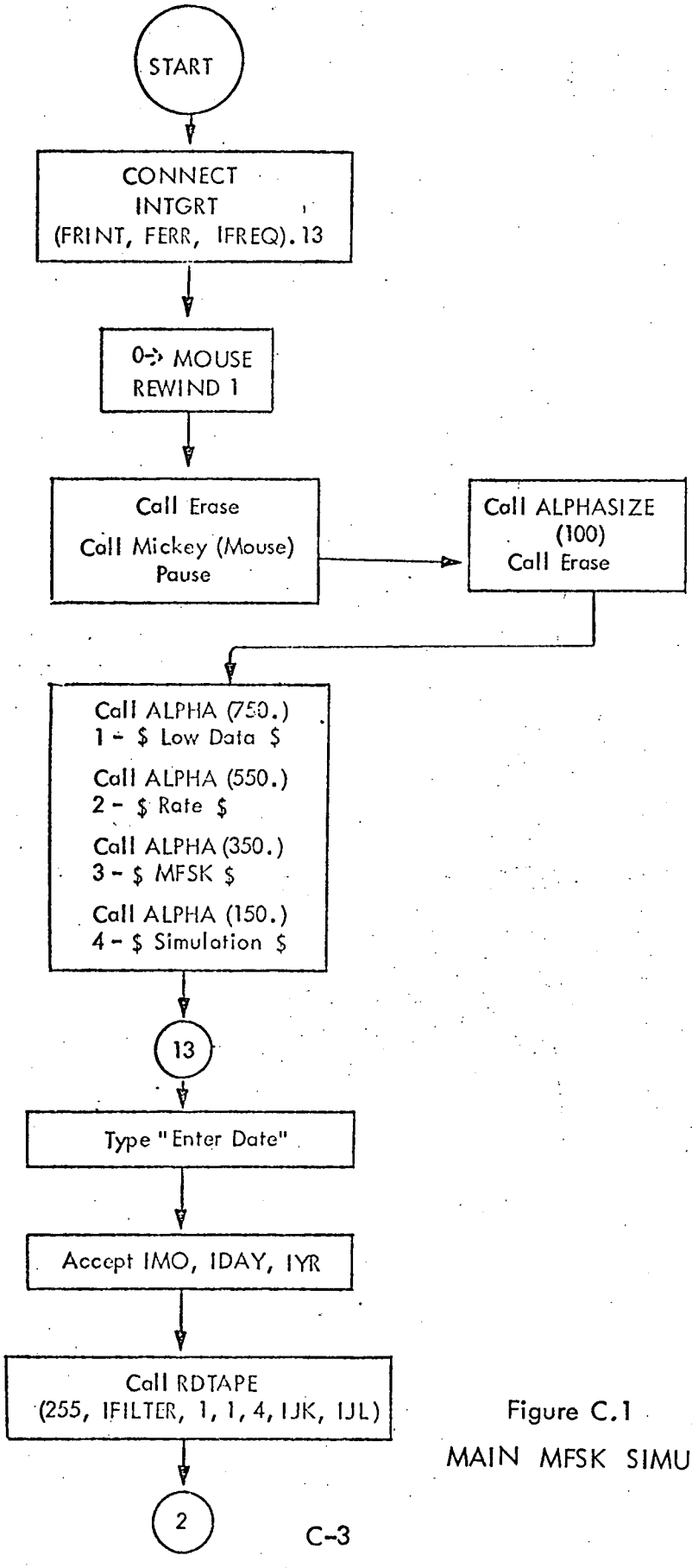

Figure C.1

MAIN MFSK SIMULATION

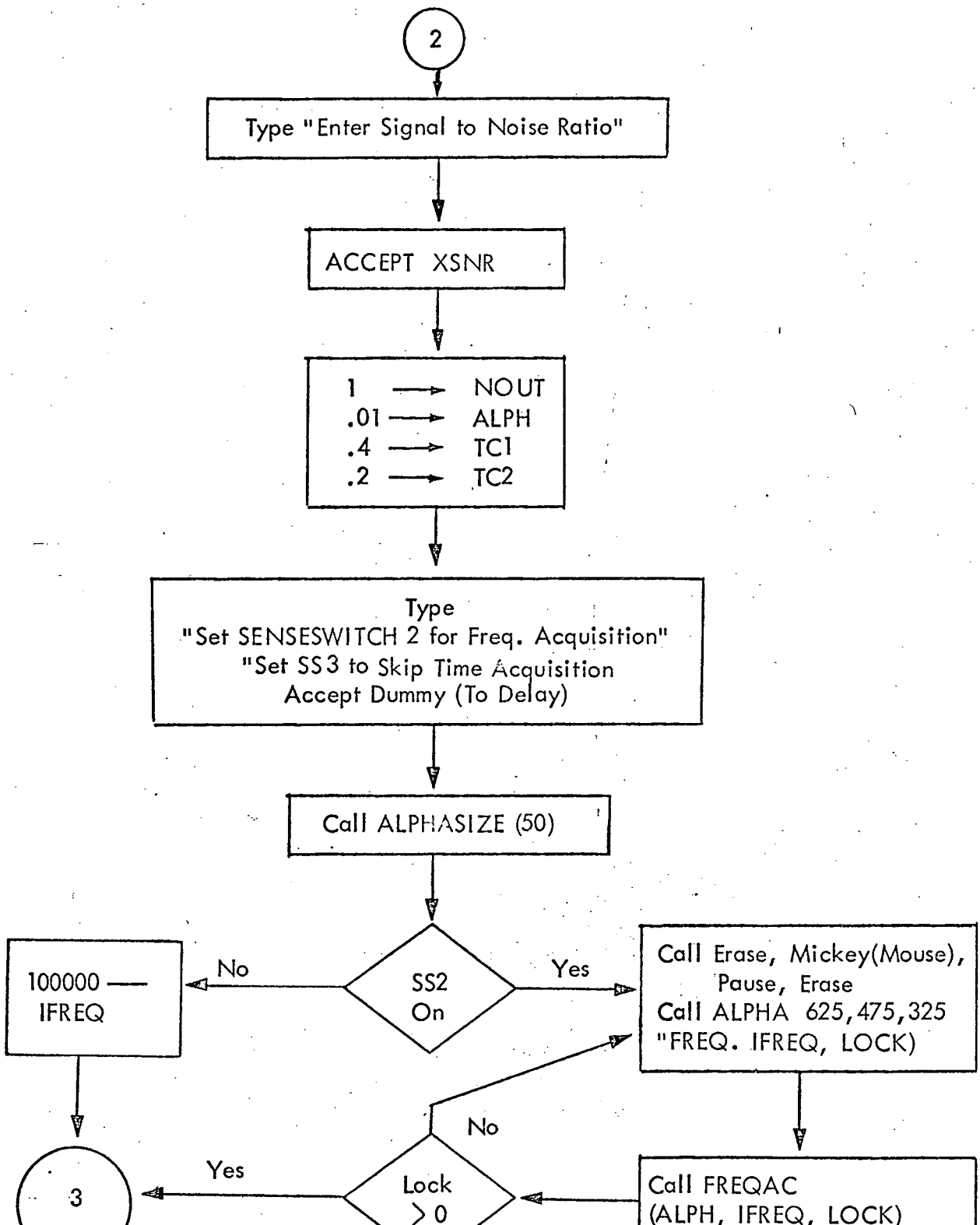

Figure C.1 (Continued)

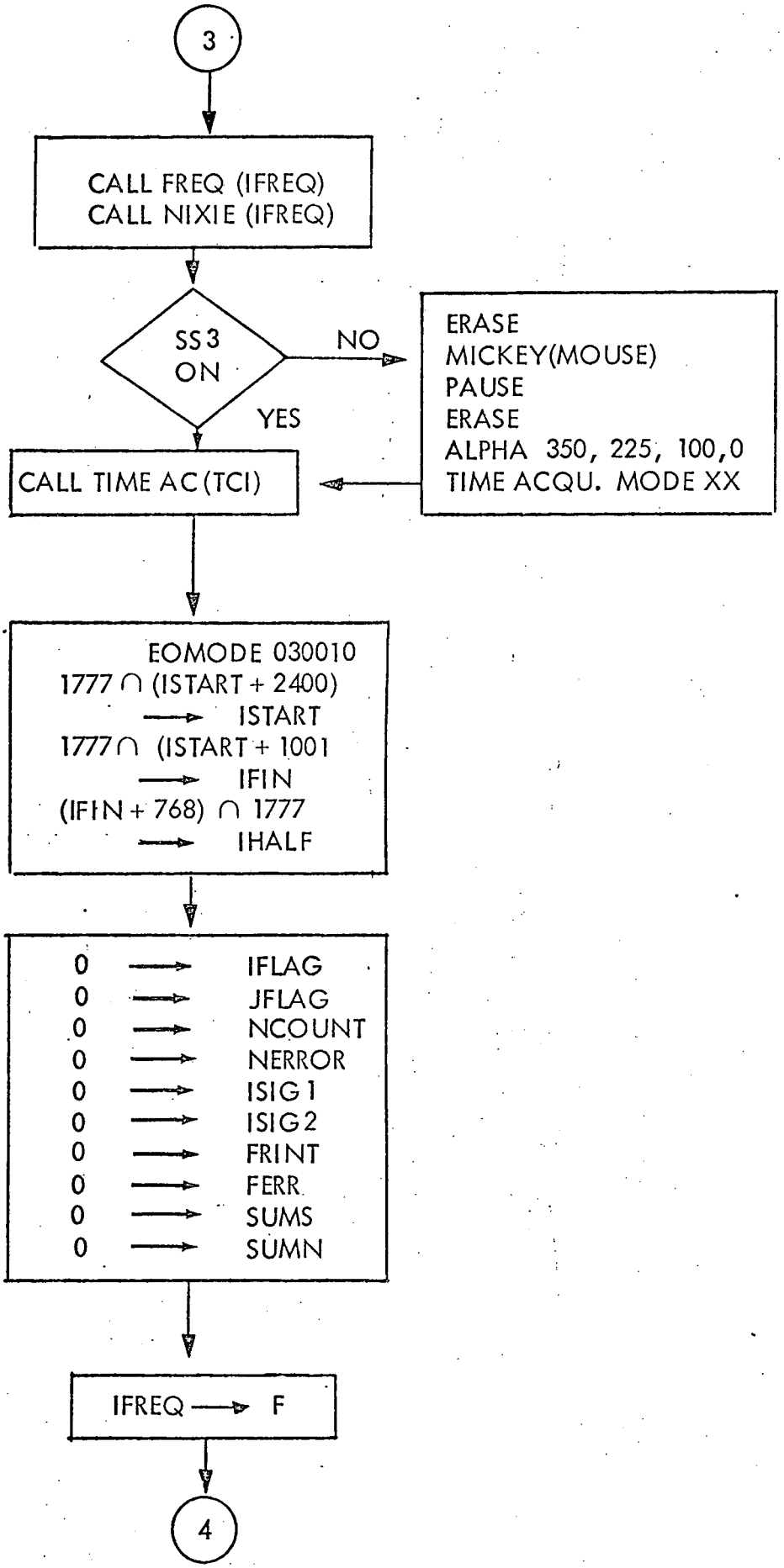

Figure C.1 (Continued)

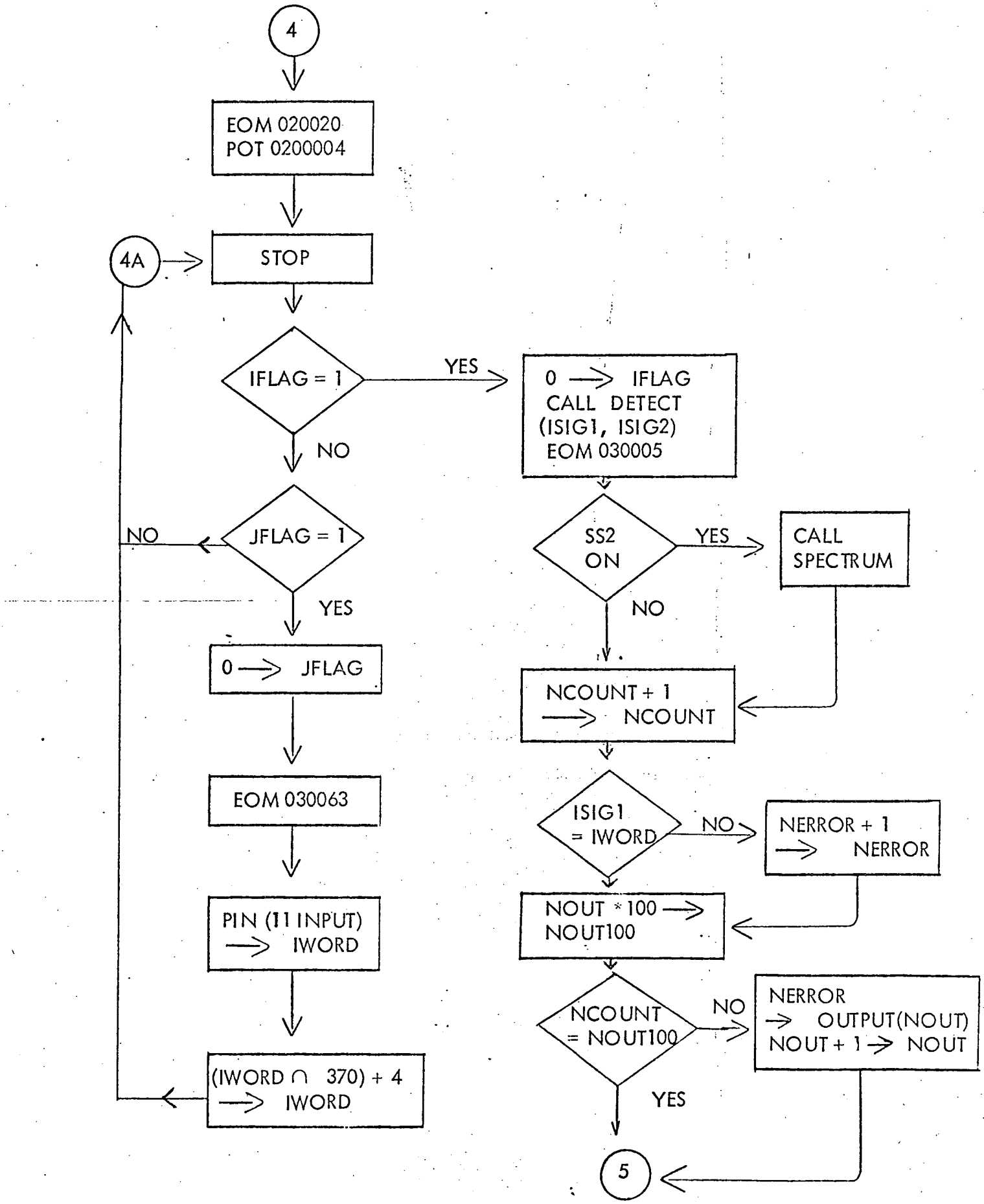

Figure C.1 (Continued)

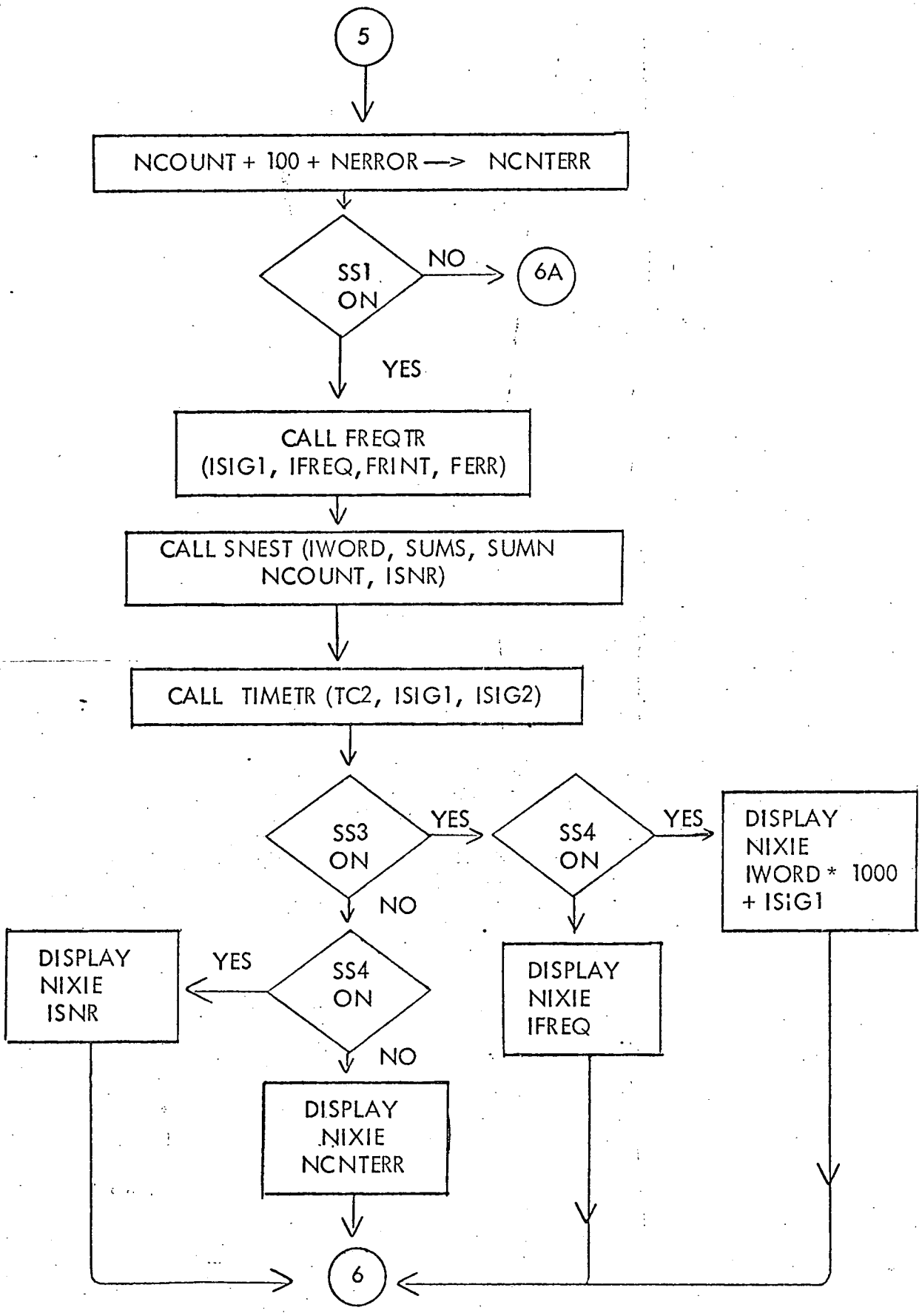

*Figure C.1 (Continued)

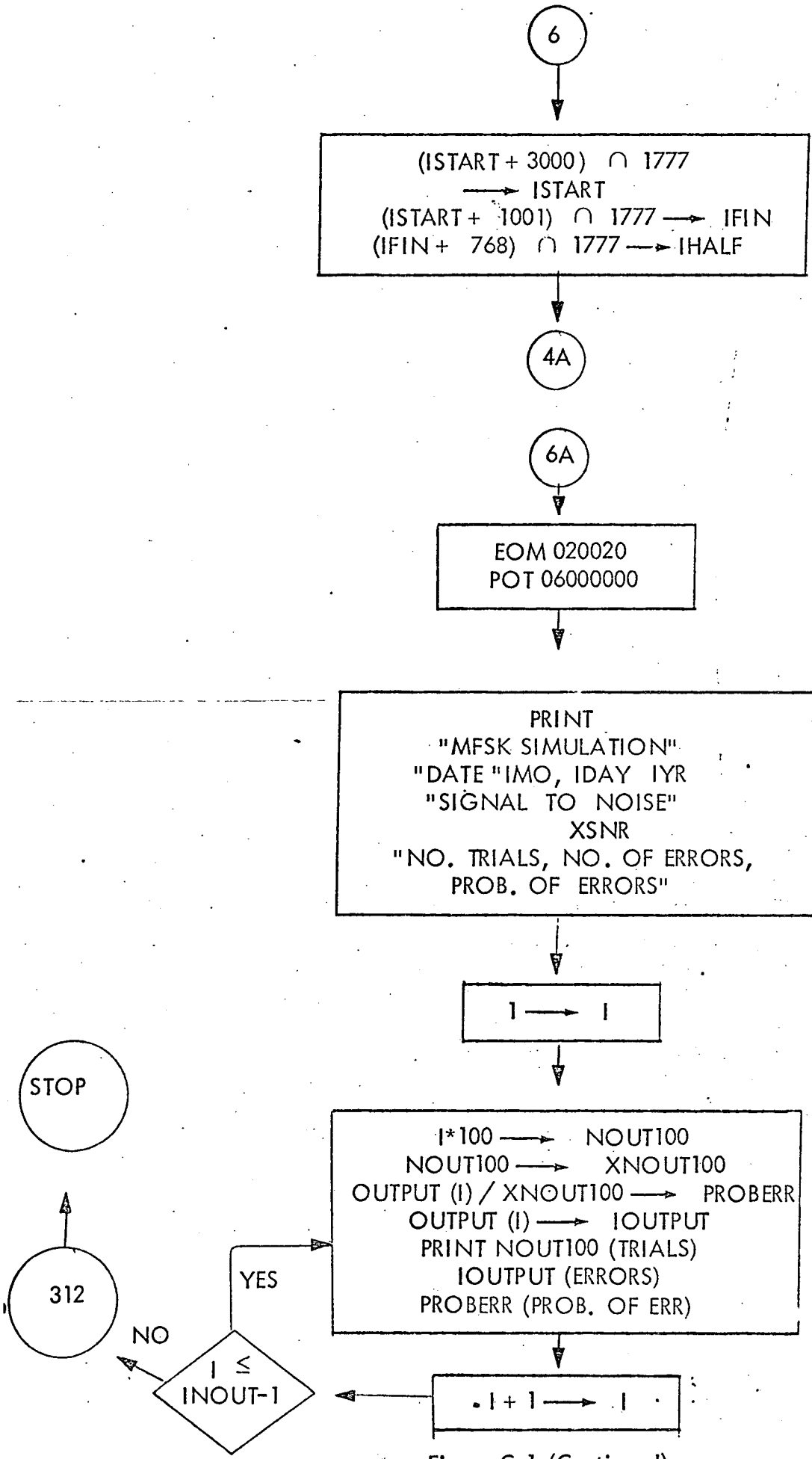

Figure C.1 (Continued)

INITIAL FREQ ACQU. SYNCHED LOC. OSC. FREQ. IS RETURNED AS INFREQ. IF LOCK IS OBTAINED, LOCK = 1; IF NOT, LOCK = 0

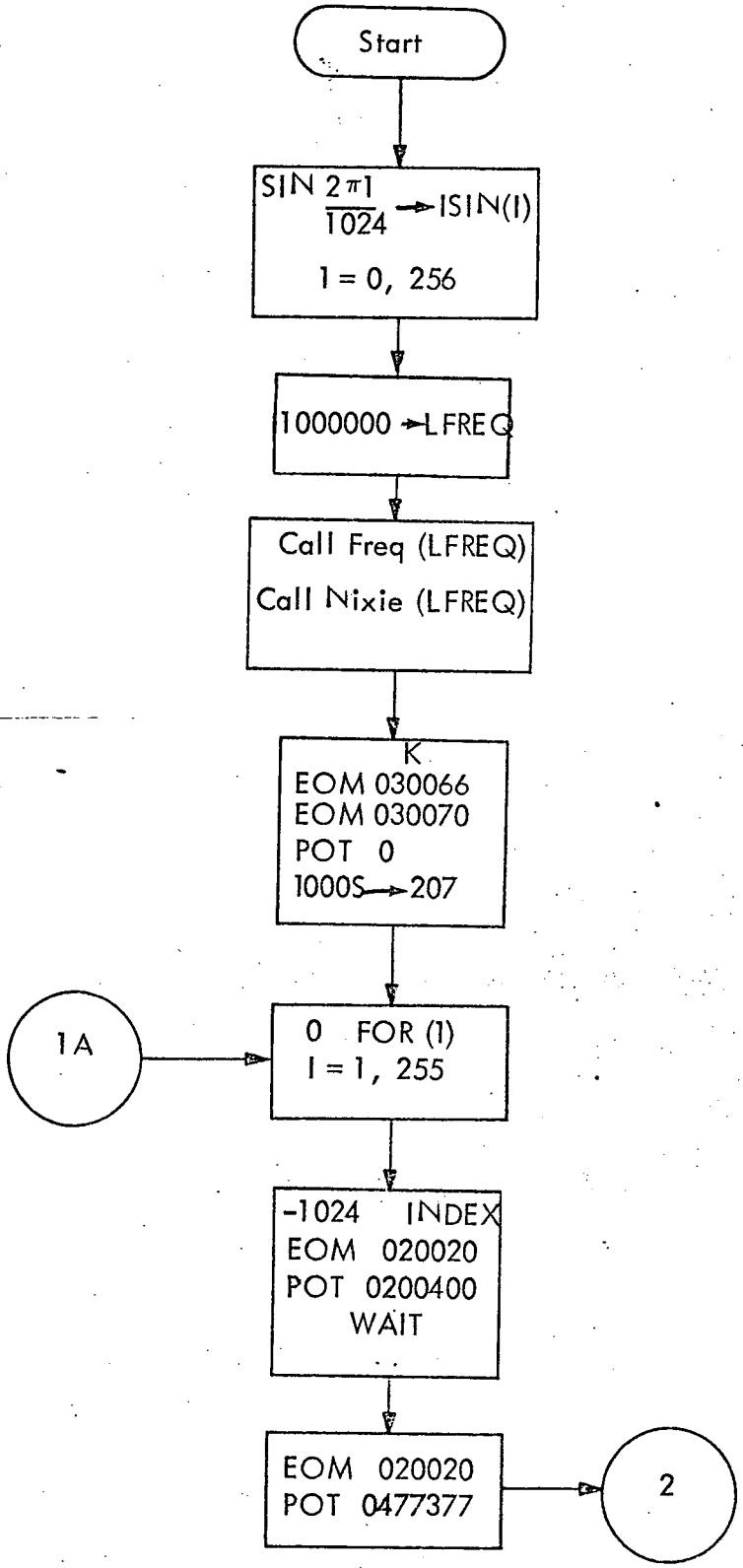

Figure C.2 FREQAC (ALPHA, IFREQ, LOCK)

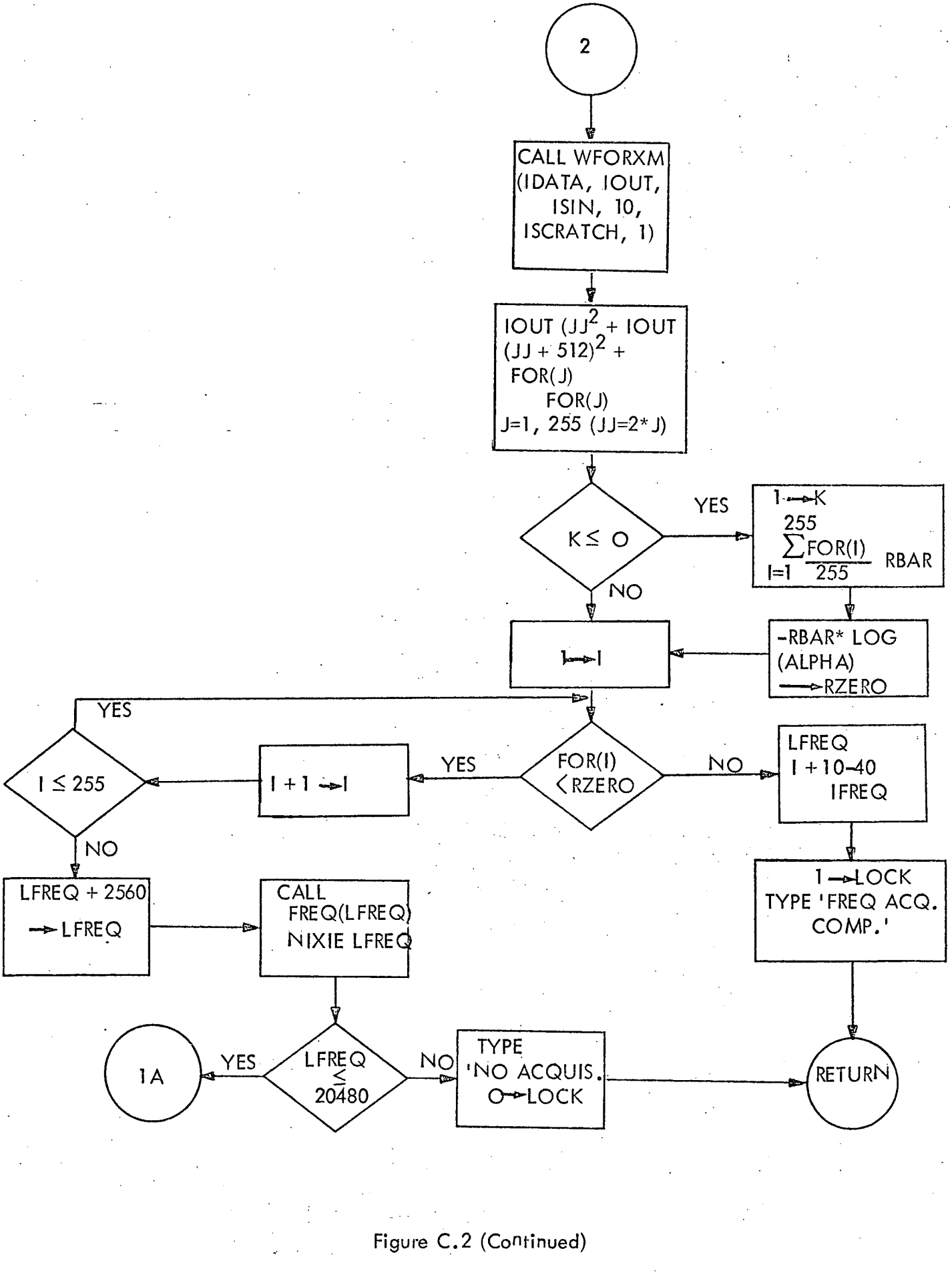

Figure C.2 (Continued)

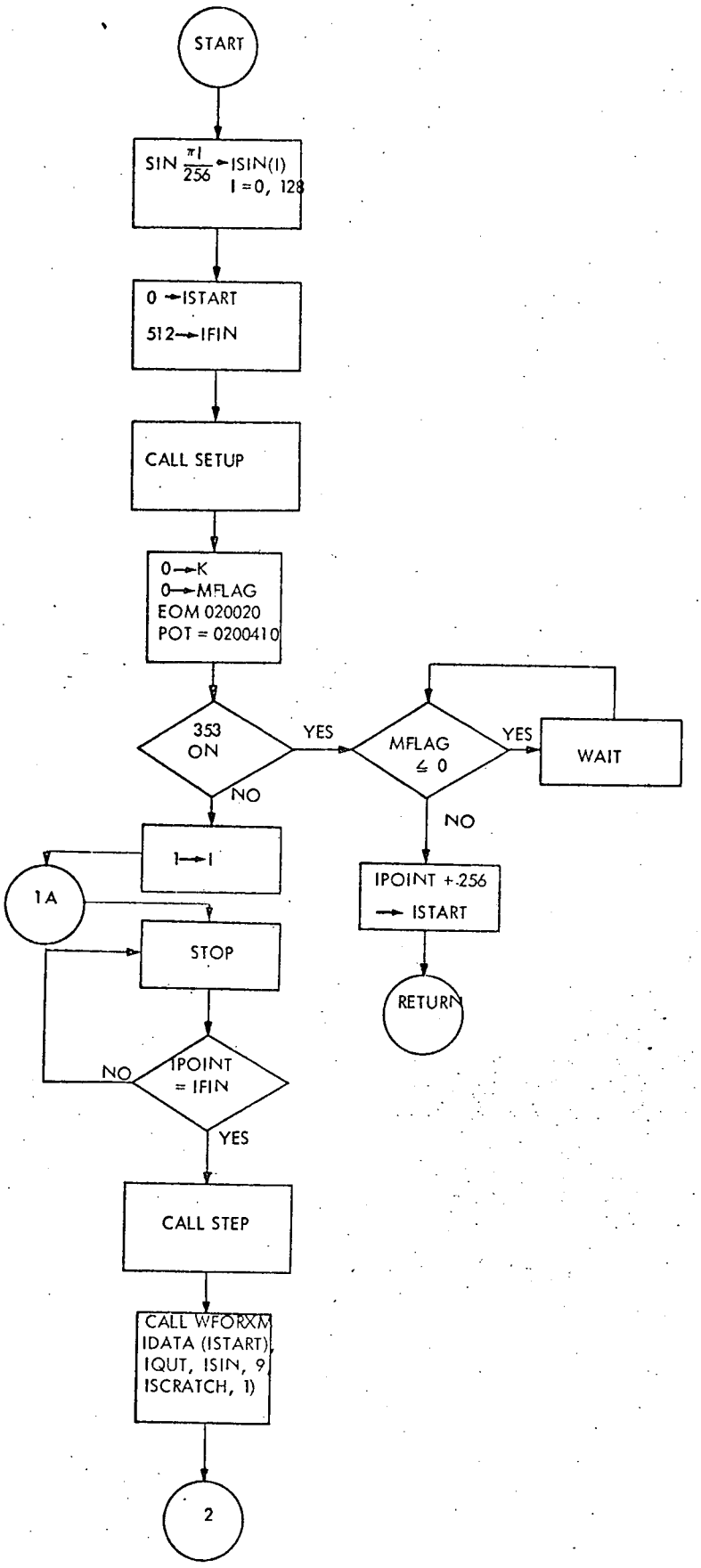

Figure C.3 TIMEAC (TCI) INITIAL TIME SYNCH AND TABLE SETUP

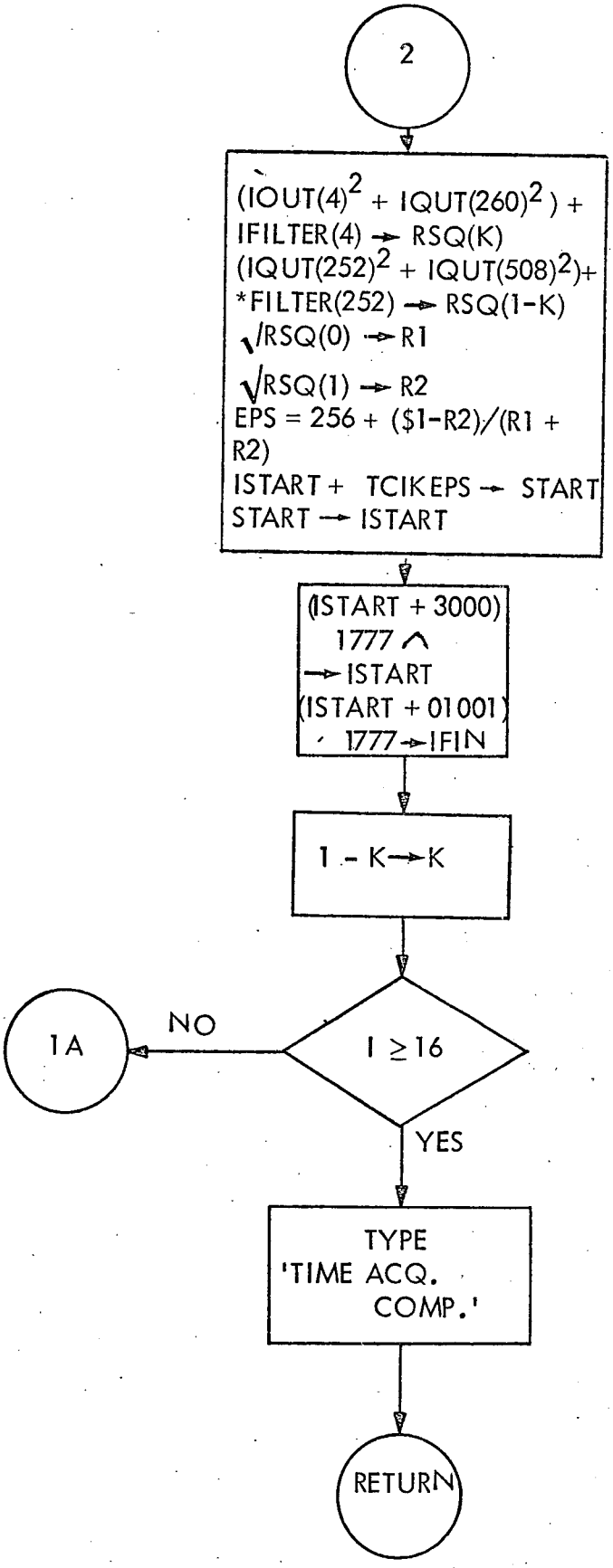

Figure C.3 (Continued)

DETERMINES LARGEST SPECTRAL COMPONENT IN THE RECEIVED SPECTRUM

ISIG1 IS THE LATEST SIGNAL
ISIG2 IS THE PREVIOUS SIGNAL

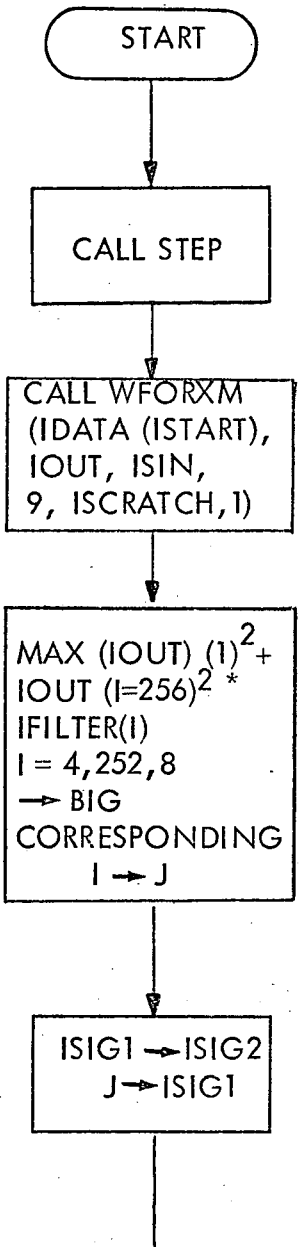

Figure C.4 DETECT (ISIG1, ISIG2)

DETERMINES LARGEST SPECTRAL COMPONENT IN THE RECEIVED SPECTRUM

ISIG1 IS THE LATEST SIGNAL
ISIG2 IS THE PREVIOUS SIGNAL

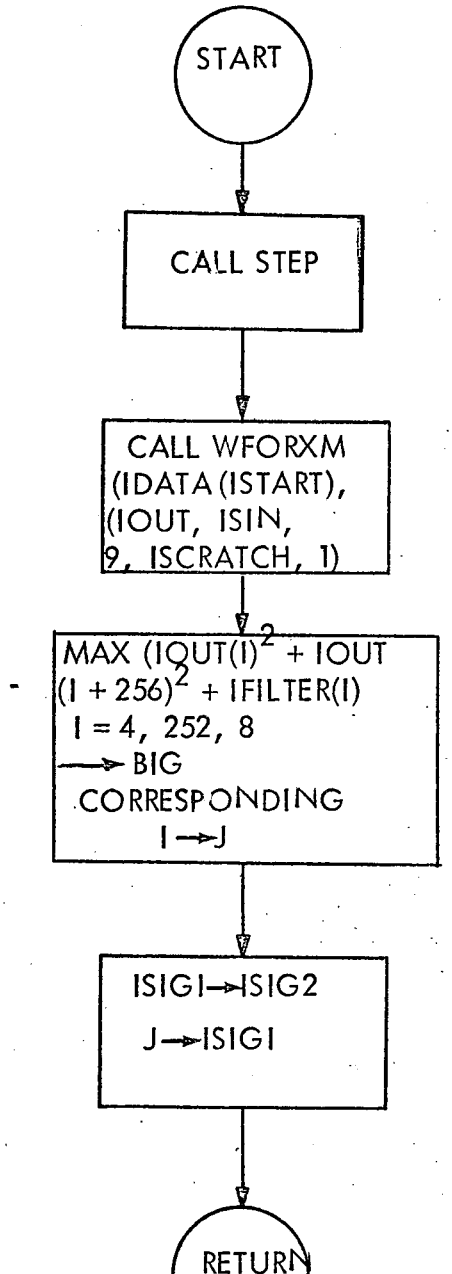

Figure C.4 (Continued) DETECT (ISIGI, ISIG2)

UPDATE FREQ. TRACK LOOP. INTEGRATION IS

PERFORMED BY THE INTEGRATE SUBROUTINE

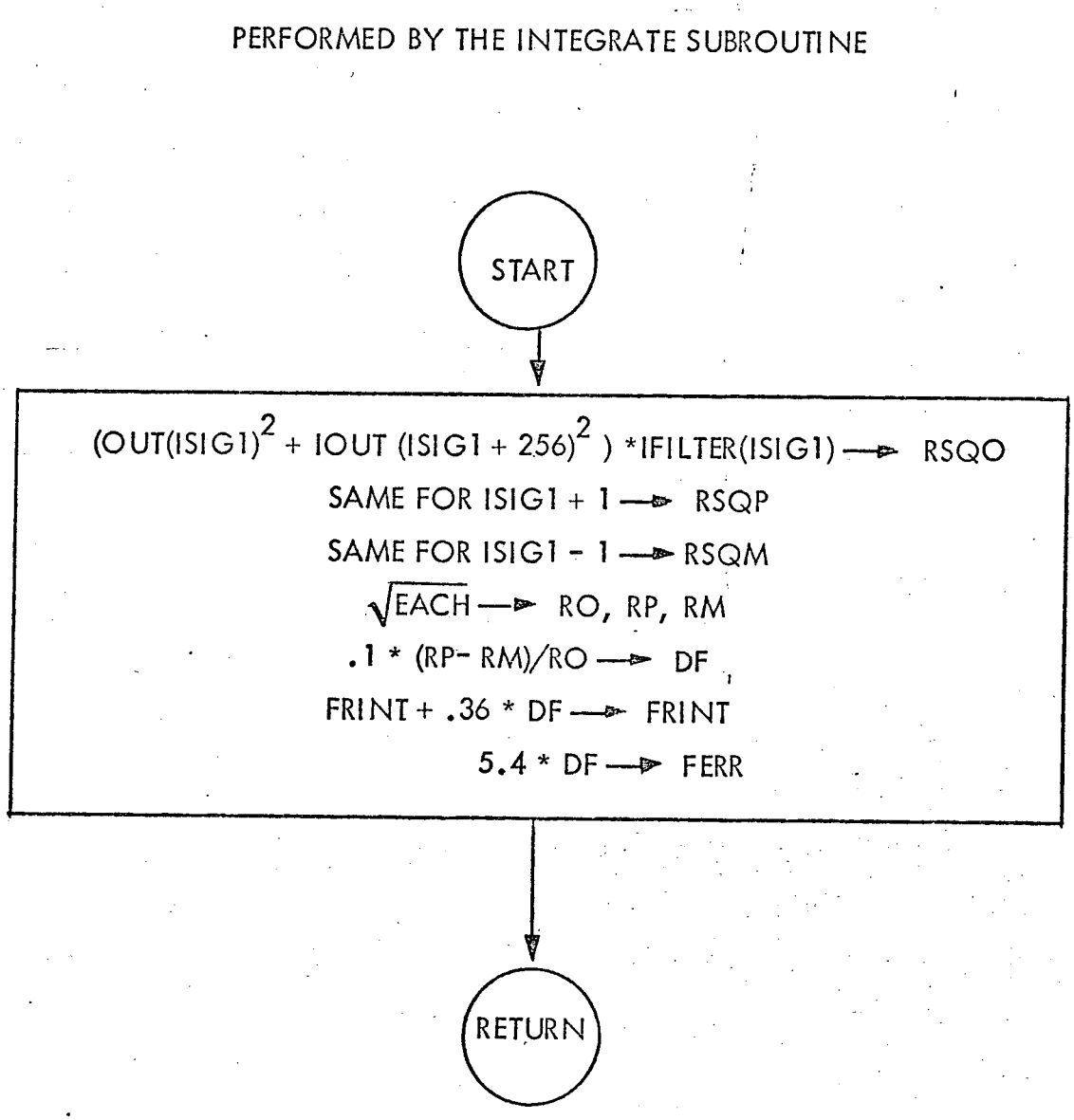

Figure C.5 FREQTR (ISIGI, IFREQ, FRINT, FERR)

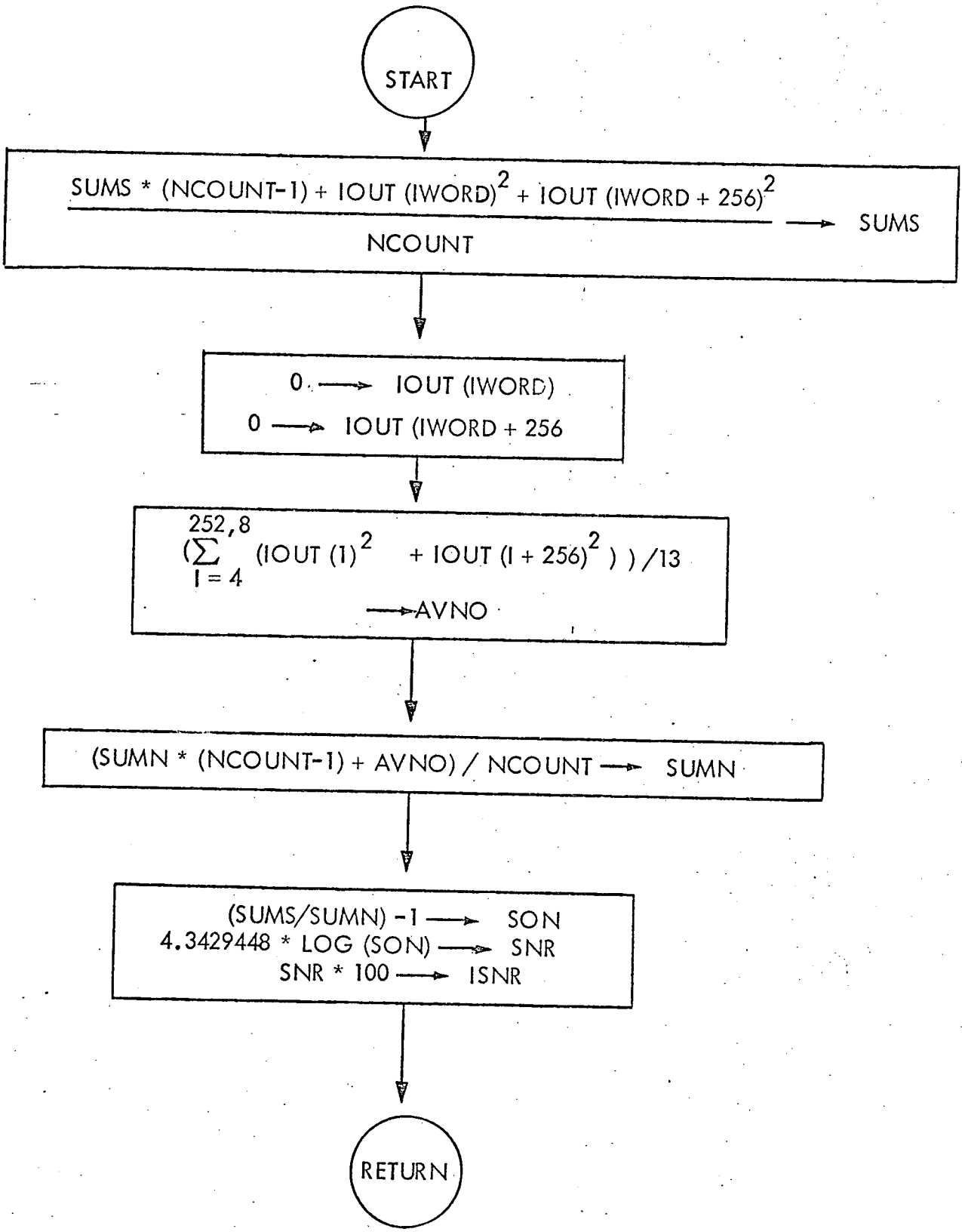

Figure C.6 SNEST (IWORD, SUMS, SUMN, NCOUNT, ISNR)

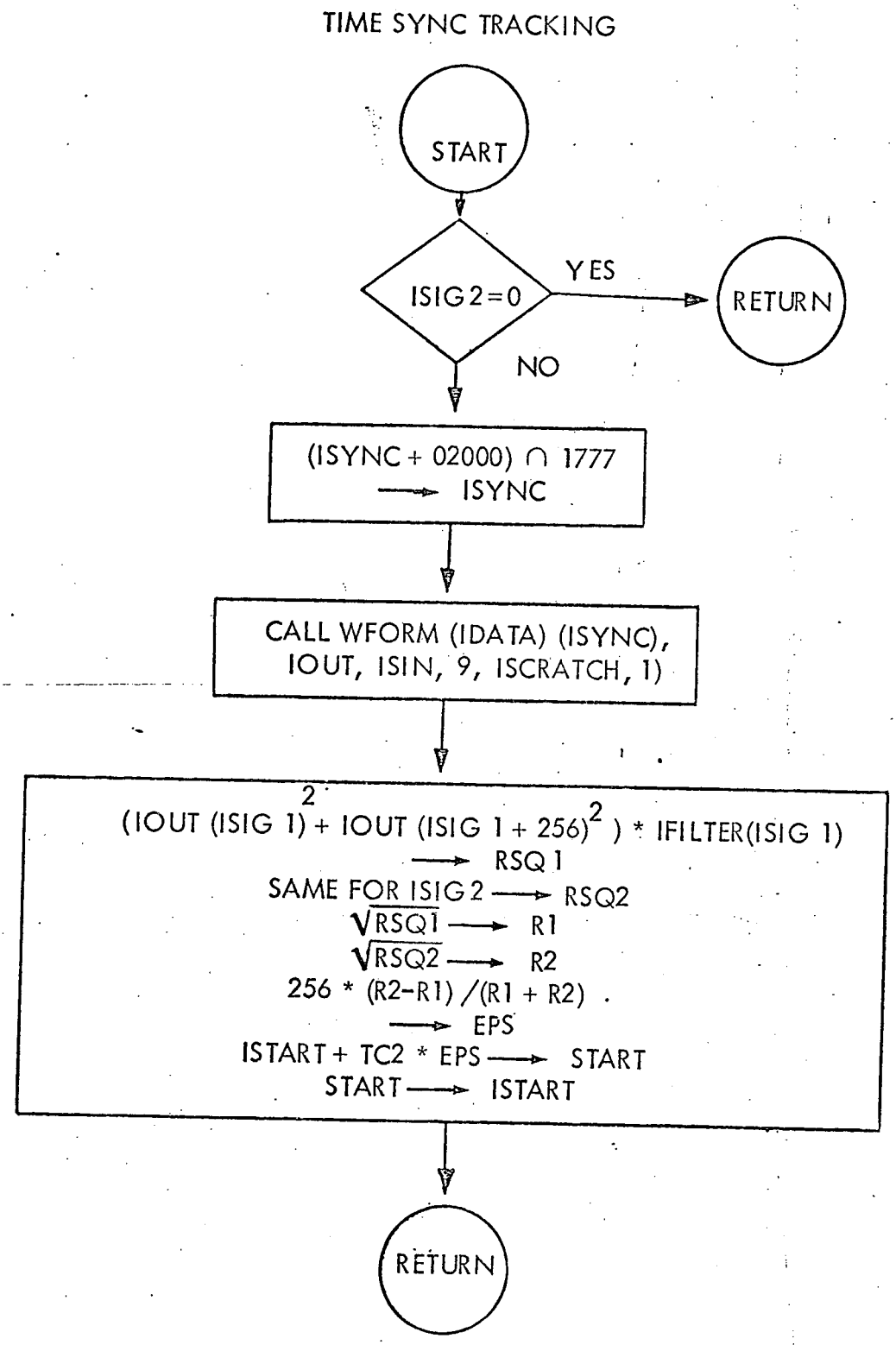

Figure C.7 TIMETR (TC2, ISIG1, ISIG2)

INTEGRATION FOR THE FREQUENCY TRACKING LOOP
RATE CONTROLLED BY INTERRUPT 215 (SET TO 1/SEC)

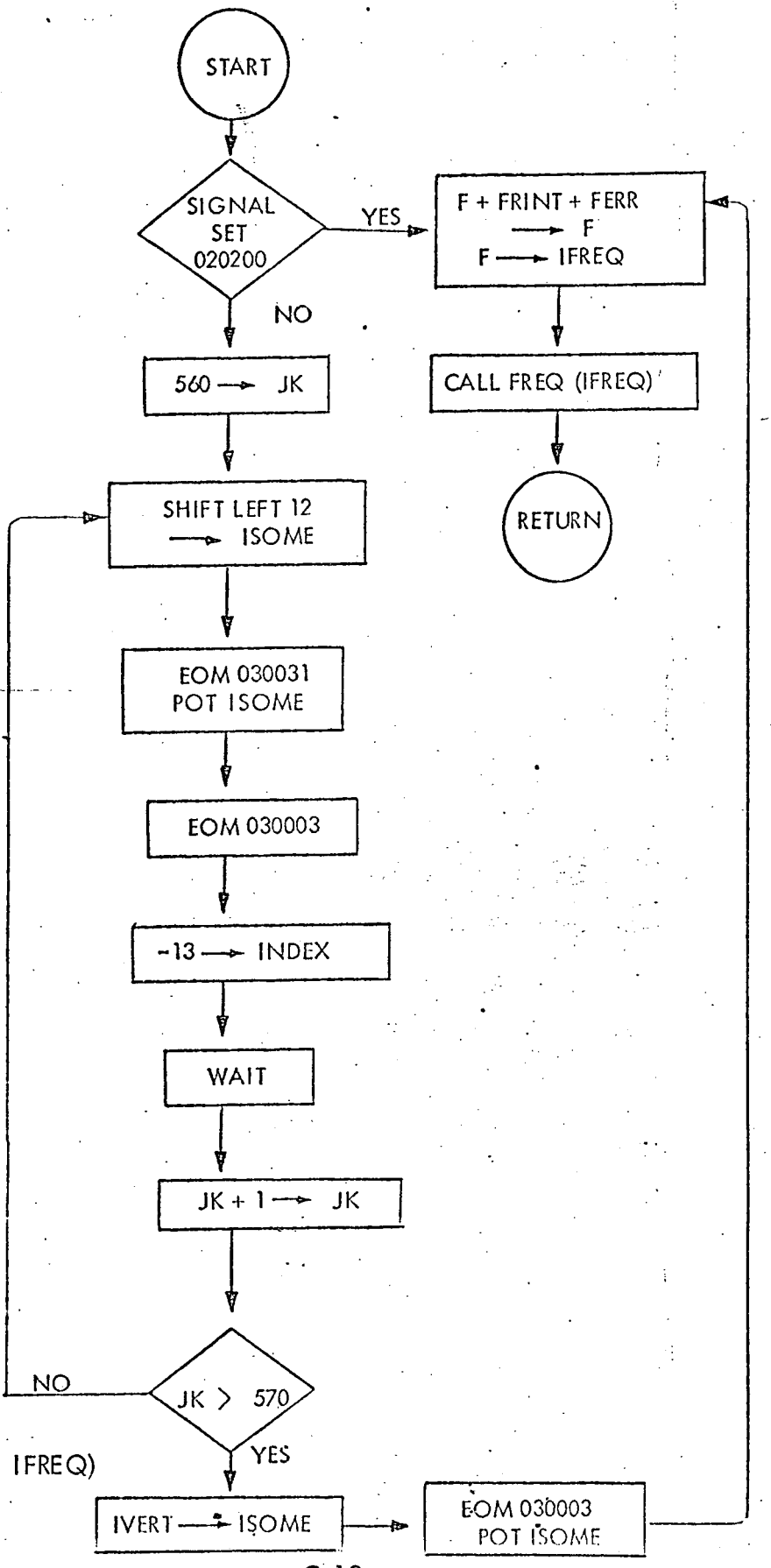

Figure C.8
INTGRT (FRINT, FERR, IFREQ)

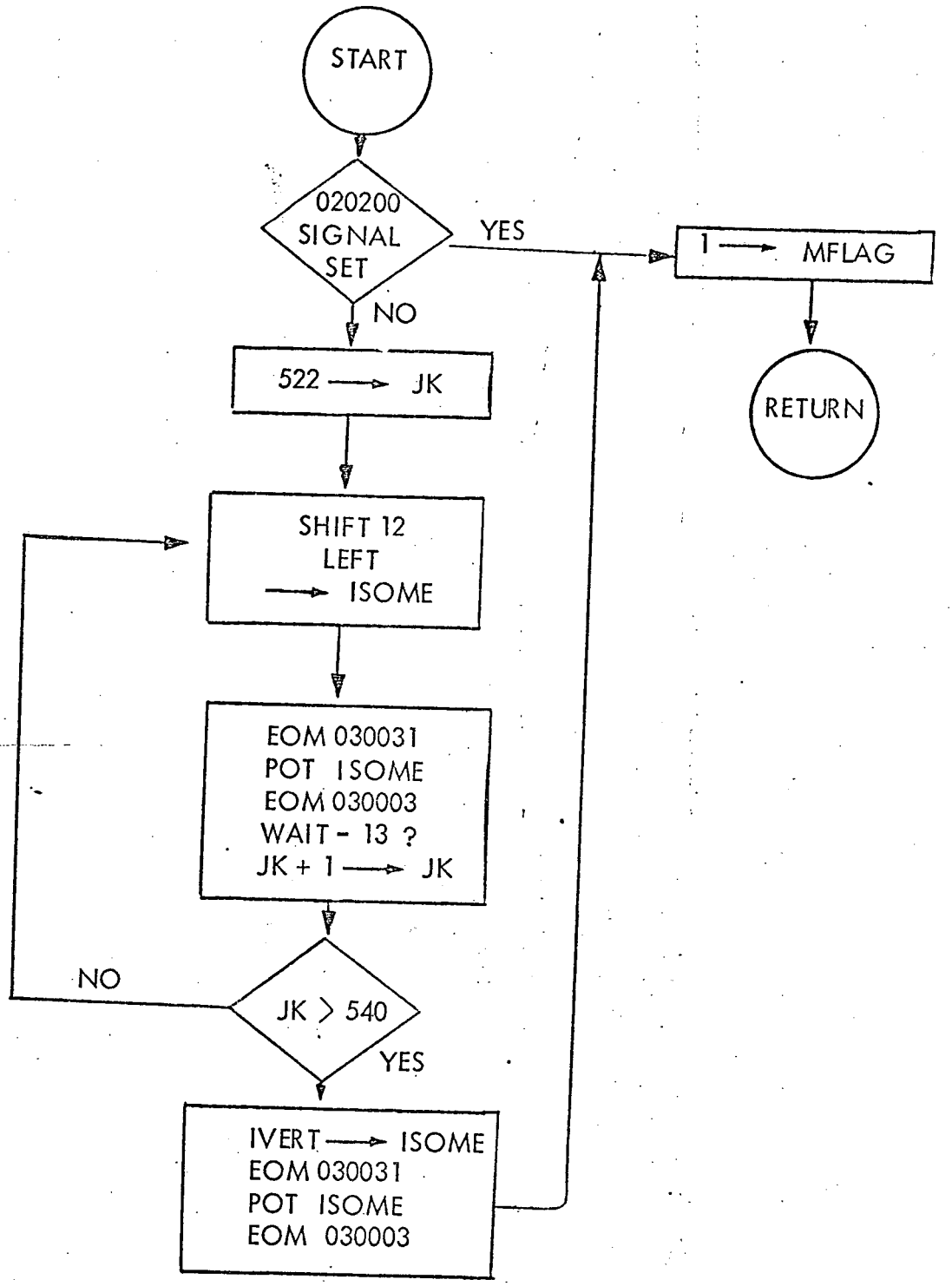

Figure C.9 BLIP

SET UP ADC, SELECT MULTIPLEX CHANNEL 0, IDATA IS CONNECTED TO THE ADC INTERRUPT.

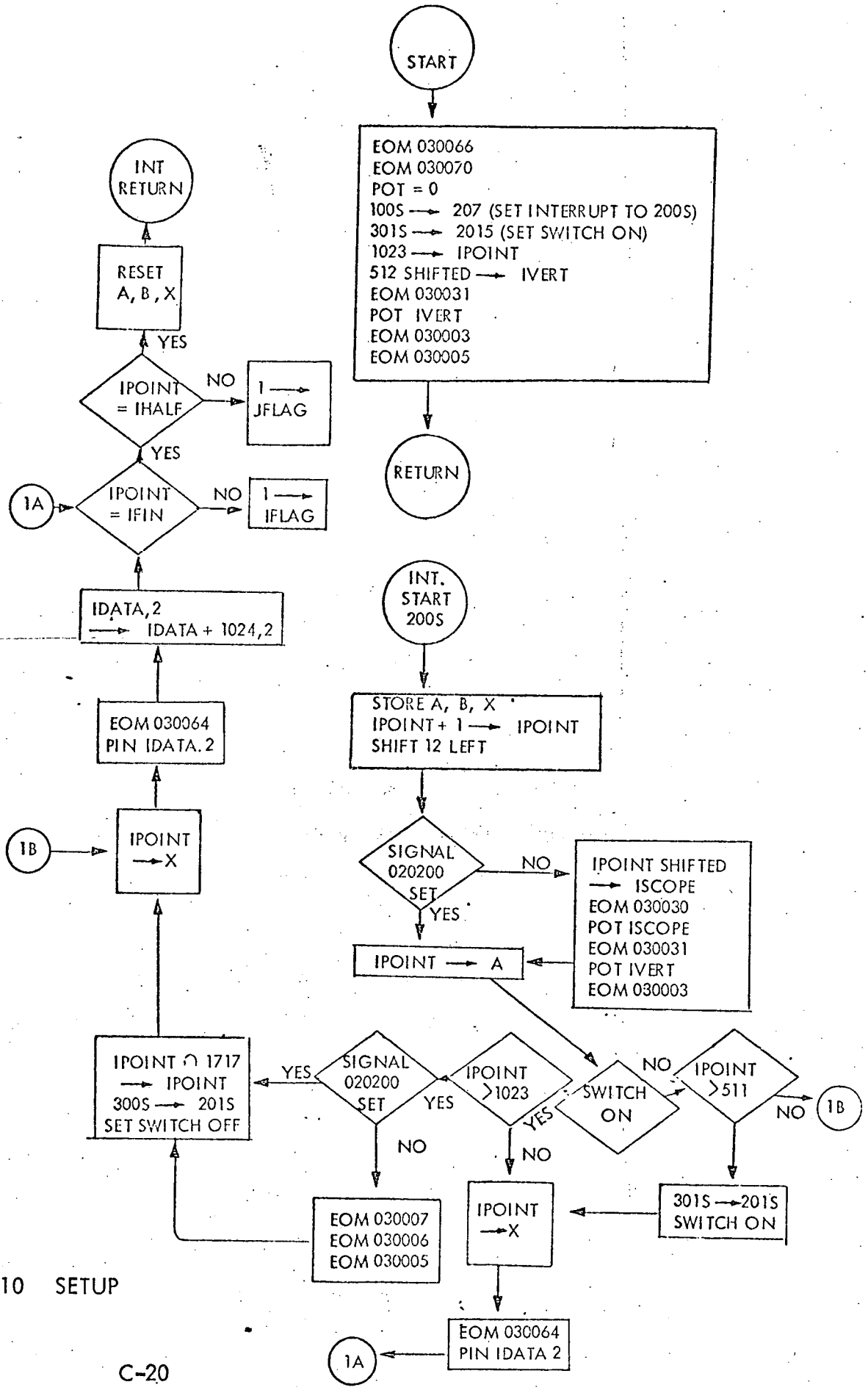

Figure C.10 SETUP

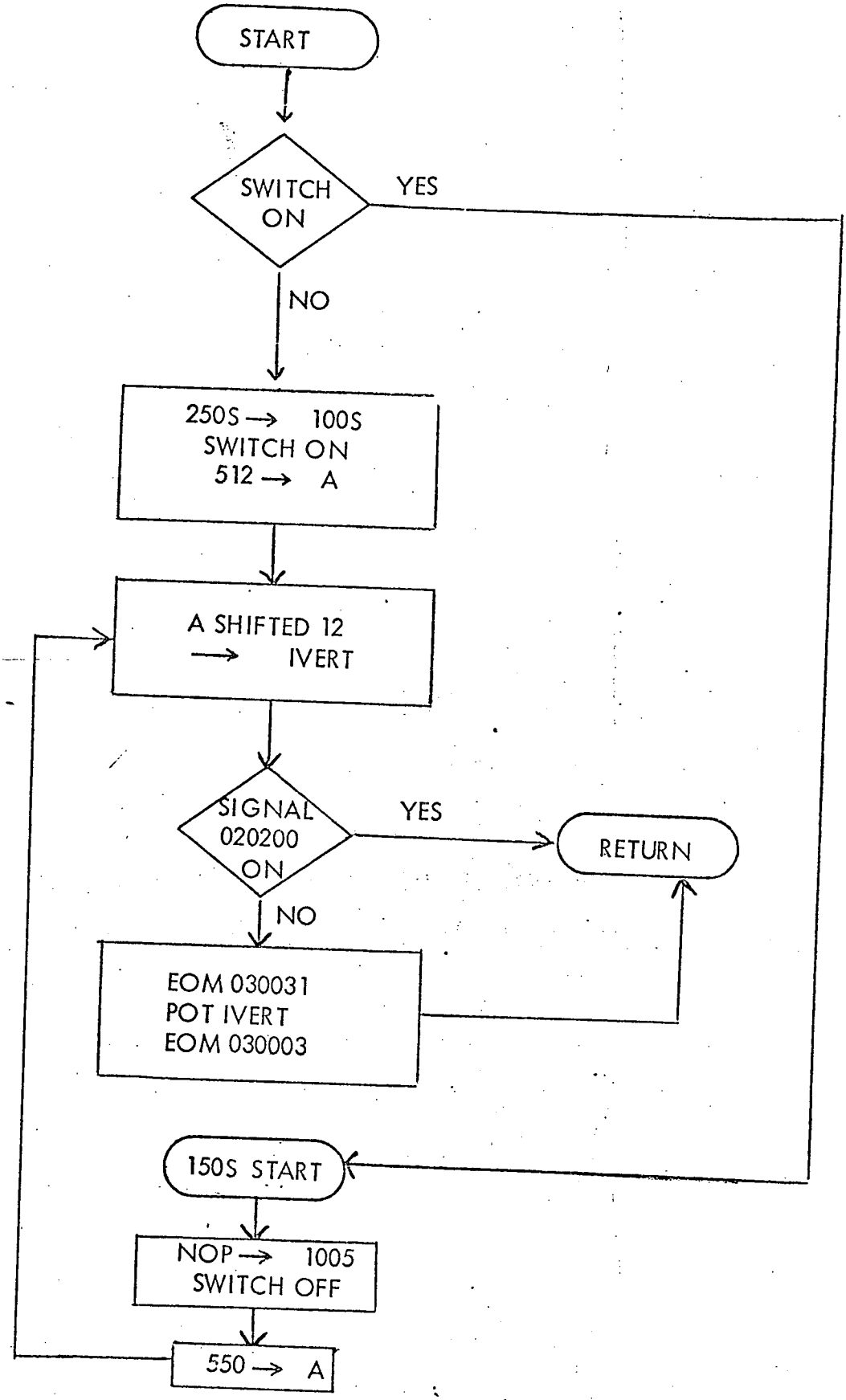

Figure C.11 STEP

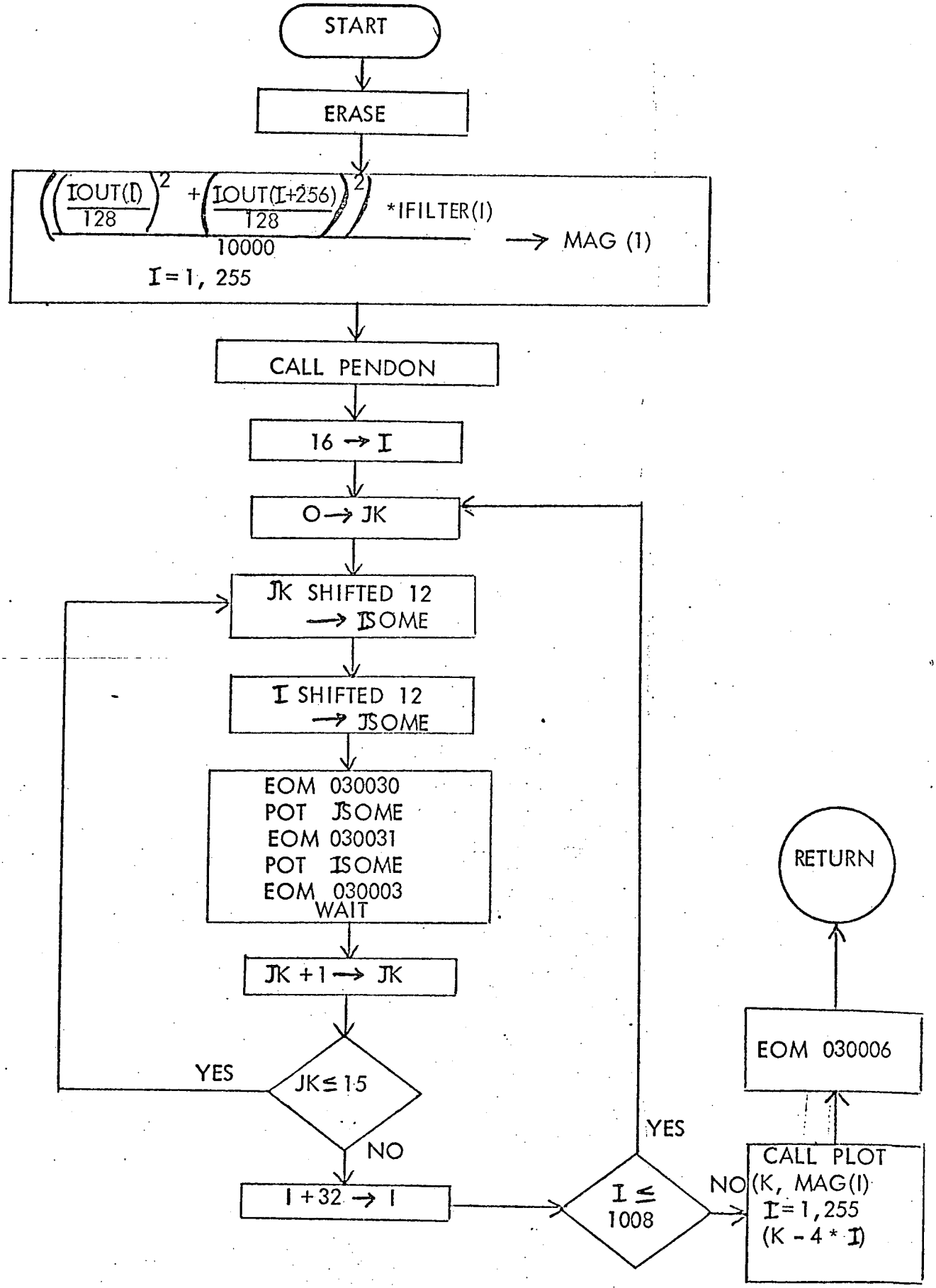

Figure C.12 SPECTRUM

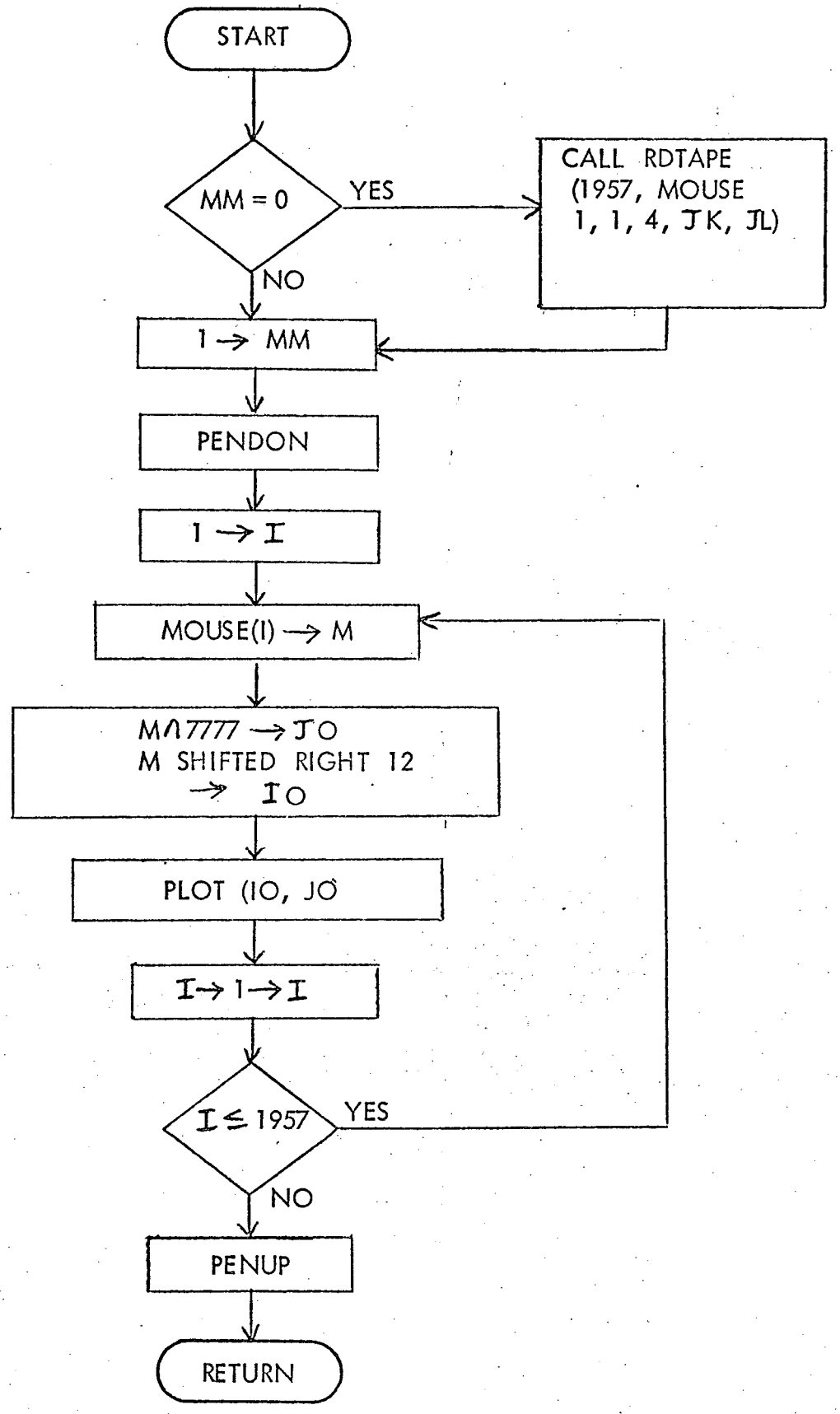

Figure C.13 MICKEY (MM)